NTNU
Norwegian University of
Science and Technology

# Anti-surge control

## Control theoretic analysis of existing anti-surge control strategies

**Terje Kvangardsnes**

Master of Science in Engineering Cybernetics
Submission date: June 2009
Supervisor: Tor Arne Johansen, ITK
Co-supervisor: Bjørnar Bøhagen, ABB AS
Jørgen Spjøtvold, ABB AS

Norwegian University of Science and Technology
Department of Engineering Cybernetics

# Problem Description

1. Review various approaches for anti-surge control using a recycle valve.
2. Establish simple dynamic model for analysis of control theoretic properties of the reviewed approaches in item 1.
    a. Neglect temperature dynamics and mole weight changes
    b. Include suction and discharge pressure dynamics
    c. Include compressor flow dynamics
    d. Include recycle line/valve flow dynamics
3. Establish simulator for item 2 in Simulink and include typical industrial implementations.
4. Analyze stability and performance of the various approaches found in item 1 using the model in item 2, and verify using the simulator in item 3.
5. Suggest tuning strategies for the various approaches.

Assignment given: 12. January 2009
Supervisor: Tor Arne Johansen, ITK

## Abstract

This report on compressor anti-surge control closes some of the gaps related to the significant properties of control strategies. Anti-surge control is an important issue in operation of e.g. oil and gas processing plants. However, control strategies have not previously been studied thoroughly from a control theoretic viewpoint. Special attention is given to the input-output relationship between recycle valve opening and control variable when changing the compressor speed. The properties are then validated through simulations.

The compression system is found to be open-loop stable for operating points along the surge control line. However, the behaviour of control variable in different points is highly dependent on control strategy. A normalized control variable structure based on a operating point invariant to inlet conditions will perform similarly for a range of compressor speeds. The report also provide greater insight in the dynamics of the compression system, along with guidelines for strategy analysis and synthesis and controller tuning.

# Preface

This thesis is the culmination of 5 years spent at the Norwegian University of Science and Technology (NTNU), studying for a MSc in Control Engineering. The problem description was given by ABB AS situated in Oslo, Norway.

Starting from scratch in January 2009, when considering insight in compressors and the field of compressor control, was a great challenge. There has been both frustrating and joyful moments during this journey. When it now all comes to an end, it is with great respect the results of my work is presented. The field of compressor control has a rich history, but hopefully some important aspects have been pointed in this thesis.

There are many people who has played important roles while I was working with the thesis. First I would like to thank the fellow students and friends Per Aaslid, Knut Ove Stenhagen, Eivind Lindeberg, Tore Brekke, Morten Dinhoff Pedersen and Lars Andreas Wennersberg. They have always been willing to discuss matters of both technical and personal character, giving valuable feedback.

The cooperation with ABB has been fruitful and I would like to thank them and my supervisors at ABB Jørgen Spjøtvold and Bjørnar Bøhagen for fascilitating my work and giving advice when needed.

Last but not least I would like to thank my family and friends for backing me up in though times, and especially my girlfriend for removing negative thoughts and stress by a gentle touch.

I am now ready to embark the ship heading for my future, applying knowledge in other environments than the academic. Even though my status as a student is cleared, I will always try to remember the words of Leonardo Da Vinci:

"Learning never exhausts the mind."

Terje Kvangardsnes Trondheim June 15th, 2009

# Contents

# List of Figures

# List of Symbols

The following list explains the symbols used in the text, unless otherwise specified. The meaning when used as subscript is marked (sub) and as a function marked (func).

| Symbol | Meaning |
|---|---|
| $a$ | framework constant |
| $A$ | cross sectional area |
| $b$ | (func) surge control line parameter |
| $c$ | constant |
| $c$ | (sub) variable related to compressor |
| $c$ | (func) surge control line |
| $C$ | Valve coefficient |
| $d$ | (sub) outlet; also desired value |
| $d$ | diameter |
| $D$ | (func) transfer function denominator |
| $e$ | (sub) equilibrium |
| $e$ | rotational speed error |
| $e$ | (func) framework disturbance |
| $f$ | (func) framework state |
| $F$ | force |
| $g$ | (func) framework input |
| $h$ | polytropic head |
| $h$ | (func) framework measurement |
| $H$ | (func) transfer function |
| $i$ | (func) framework control variable (measurement) |
| $j$ | (func) surge line |
| $J$ | inertia |
| $k$ | ratio of specific heat |
| $k$ | (func) framework control variable (states) |
| $K$ | PID gains; also transfer function gain |
| $l$ | recycle valve opening |
| $L$ | length; also Lie derivative operator |

| | |
|---|---|
| $m$ | (sub) measured variable |
| $m$ | mass |
| $m$ | (func) double derivative of control variable |
| $M$ | molar mass |
| $N$ | rotational speed (rpm) |
| $N$ | (func) transfer function numerator |
| $o$ | (sub) orifice |
| $p$ | pressure |
| $q$ | volumetric flow |
| $r$ | radius |
| $r$ | (sub) variable related to recycle flow; also corrected or reduced variable |
| $R$ | with subscript denotes ratio; otherwise universal gas constant |
| $s$ | (sub) inlet |
| $t$ | (sub) variable related to check valve |
| $T$ | temperature |
| $u$ | framework system input |
| $v$ | framework disturbance; also fluid flow velocity |
| $v$ | (sub) property related to valve |
| $V$ | volume |
| $w$ | mass flow |
| $x$ | framework state |
| $y$ | framework measurement |
| $z$ | framework control variable |
| $Z$ | compressibility |
| $\alpha$ | real part of complex number |
| $\beta$ | imaginary part of complex number |
| $\rho$ | density |
| $\sigma$ | polytropic compression exponent |
| $\tau$ | torque |
| $\Psi$ | (func) compressor characteristics |
| $\psi$ | (func) framework compressor characteristics |

# Chapter 1

# Introduction

## 1.1 Compressors

The compressor is a mechanical device whose aim is to increase the pressure of a fluid. The term compressor is mostly used for for applications where the fluid is in gas state, whereas the term pump is used for increasing pressure in liquids.

How the pressure increase is achieved, depends on the type of compressor. Some increase pressure by reducing the volume occupied by the gas, e.g. reciprocating compressors, scroll compressors and diaphragm compressors. Others work by first increasing fluid velocity, followed by a reduction of velocity to increase the fluid pressure due theory of energy conservation. If the fluid velocity is reduced without dissipating energy, kinetic energy will be transformed into potential energy. Concerning gases, the increase in potential energy manifests as both an increase in pressure and density.

Turbo compressors, hereunder axial and centrifugal/radial compressors, work by the latter principle. Energy is transferred to the fluid by a drive unit which is connected to rotating blades called the impeller. This causes the fluid to accelerate, before it enters a stationary passage, the diffuser, where the fluid is decelerated.

The terms axial and radial are related to which direction the fluid flows through the impeller. The fluid flow in axial compressor is more or less parallell to the rotating axis of the compressor. For centrifugal compressors, fluid leaves the impeller radially to the rotating axis.

Compressors are used in a wide range of applications. Axial compressors are preferred where large flow rates or small physical dimensions are required. Centrifugal compressors on the other hand, are able to operate at higher pressures and are more resistant to erosive, dirty and corrosive gases. Examples of applications are:

- Gas transport
- Refrigerators and air conditioners
- Turbochargers for combustion engines

- Storage of air in containers e.g. for diving gear

Regardless of applications, turbo compressors may experience instability problems related to their operating conditions. These instabilities are unwanted because they may lead to destruction of nearby equipment or the compressor itself, and can be avoided by ensuring that enough fluid flows through the compressor. One way of achieving minimum flow is to lead fluid from compressor outlet to compressor inlet, or in other terms through fluid recycling. Recycle flow is regulated by a recycle valve. The state of the art protection schemes also stabilize the compressor operation through active control of e.g. compressor rotational speed. However, in industrial application the simple, yet energy inefficient, recycling scheme is widely used to protect the compressor and its surroundings.

## 1.2 Motivation

Even though the recycling scheme is old and the technology mature, there is a lack of studies where control theoretic analysis tools have been used to study the dynamics of the compression system including the recycle line. Further, as the recycle valve opening often is determined by a simple PID controller with constant gains, the linearity of control strategy is of importance. There are a variety of ways to synthesise the control variable used as input to the controller, and a few of these strategies will be analyzed in terms of its behaviour in different compressor operating points.

## 1.3 Report organization

In chapter 2, theory related to the centrifugal compressor and its performance is presented. Especially the instability phenomenon called surge is thoroughly described. The chapter also contains a section presenting various compressor control schemes and means to achieve control.

Chapter 3 presents a compression system model, and further adapts this model to a framework suited for control theoretic analysis. Some general considerations regarding the model properties and equilibria are also stated.

The analysis of the compression system and control strategies is given in chapter 4. First, the characteristics for different parts of a control strategy are identified, and general remarks concerning these characteristics presented. Then, two different control strategies are analyzed, both related to the presented characteristics and their dynamic behaviour.

In chapter 5, simulations of the compression system models are performed to validate results from the control theoretic and structural analyses.

# Chapter 2

# Theory

The field of compressor control embrace a range of concepts which are essential for understanding the motivation behind different control strategies. The most important of these concepts will be presented in the following chapter.

## 2.1 Centrifugal compressor

The compressor used further in this thesis is the centrifugal compressor, and a more detailed decription of its main characteristics follows. For further reading consult e.g. [1].

The centrifugal compressor is, as mentioned, characterized by a radial flow at the impeller exit. A principal sketch of one type of centrifugal compressor and its components is shown in Figure 2.1. Fluid enters the compressor through the inlet nozzle, which essentially is a pipe leading the fluid into the compressor. Inlet guide vanes or blades may be mounted inside the nozzle, such that the fluid rotates before entering the impeller. These guide vanes can also be adjustable and used for compressor control.

The part of the impeller which penetrate the inlet nozzle end, is called the inducer. Here, the inducer blades are angled toward the direction of rotation. In the inducer the fluid's angular momentum is increased without increasing its radius of rotation. In the centrifugal section of the impeller, fluid enter from the inducer and exit the impeller radially. The blades at the exit may be curved in a backward- or forward swept manner, away from or against the angle of rotation. Figure 2.1 shows an impeller with straight blades, also called a radial vaned impeller.

From the impeller, the fluid flows into the diffuser, where the velocity is reduced in order to gain pressure. The diffuser channels are therefore usually diverging. Pressure increase also occur due to redirection of flow. Vaned diffusers are chategorized by their geometry, e.g. airfoil vanes and island vanes. The latter type is shown in Figure 2.1. Similar to the inlet guide vanes, diffuser vanes may also be adjustable.

The last major part of the compressor is the volute or collector, which gather the fluid leaving the diffuser and deliver it to the compressor outlet pipe. The

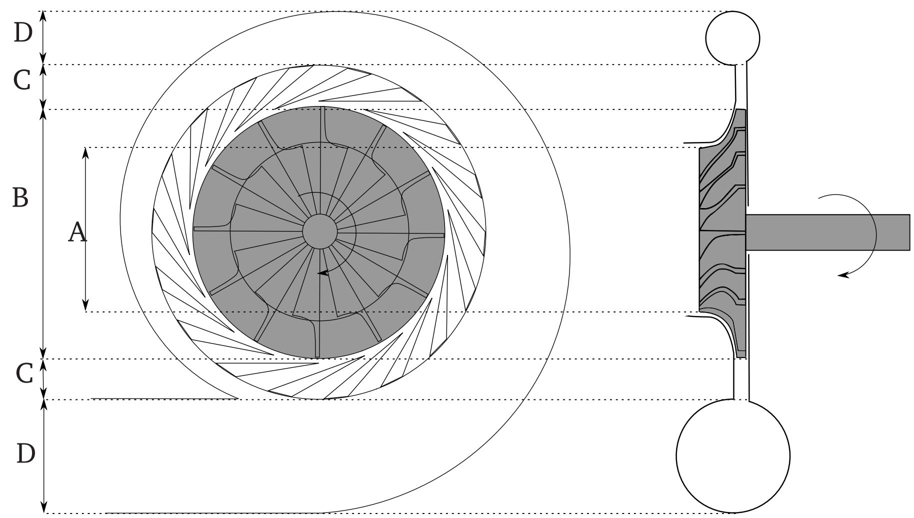


**Figure 2.1:** Compressor components shown from front and side where A: inducer B: impeller C: diffuser D: collector, and rotating parts are colored grey, and the arrows indicate the direction of rotation.

collector, like the diffusor channels, have an increases in the cross sectional area such that fluid kinetic energy converts into pressure.

Centrifugal compressors may also have several stages, where two or more impellers are mounted on the same drive shaft. Fluid flows from one impeller to the next via diffusors and collectors. Consequently, a series of single stage compressors constitute the multi stage compressor. A multi stage compressor is able to produce the same pressure increase as that from a single stage compressor with significantly larger impeller.

Compressors are often driven by electric motors or gas turbines. Electric drive units are generally easier to control and have quicker response. However, for applications where use of electric power is impossible or undesireable, gas turbines may be employed as drive units. Especially natural gas compressors are highly suitable for gas turbine drives, as the compression medium also fuels the compression system.

### 2.1.1 Compressor maps

Compressor performance capabilities are usually visualized by compressor maps or charts, which describe the relationships between the compressor's characteristic variables. The relationships are valid in steady state conditions. According to [2], four variables are needed to define the fundamental compressor characteristics. The choice of these variables is, among others, dependent on the scope of the viewer, producer preferences and traditions. Regardlessly, the characteristic variables are related to:

- Compressor speed.
- Flow through compressor.

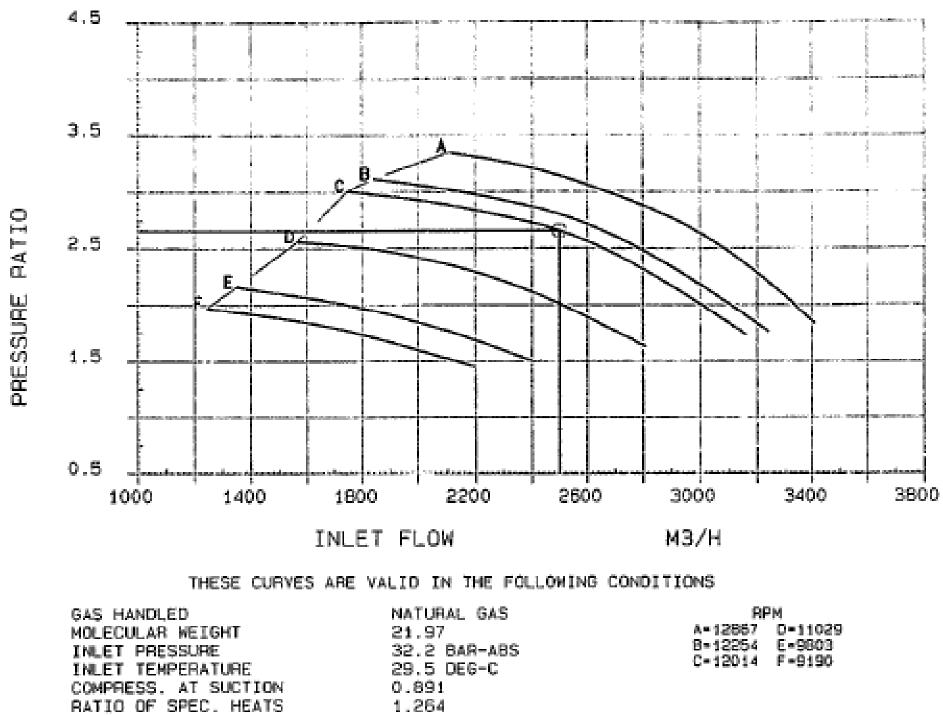


**Figure 2.2:** Example of compressor map.

- Pressure rise [1].
- Energy efficiency.

An example compressor map is given in Figure 2.2, where the variable representing energy efficiency is omitted.

### 2.1.2 Surge

Both axial and centrifugal compressor are subjected to different phenomena limiting their operational range. The stonewall or choke phenomenon is characterized by fluid flowing through the compressor without any net increase in pressure, caused by a low load or discharge pressure. At this point, the flow resistance through the compressor equals the energy increase of the gas. The rotating stall phenomenon is in many ways the opposite, where fluid flow oscillates around zero with an increase in pressure. However, rotating stall is usually referred to as local behaviour, only occuring in regions of the compressor while the net flow through the compressor is positive. But the most severe phenomenon when regarding compressor operational contraints is known as surge, characterized by oscillations in all of the compressor characteristic variables.

Rotating stall may develop such that flow oscillates in every part of the annular flow through the compressor. If no means are employed to counteract the

[1] By pressure rise is meant a general increase in pressure, not the special increase given by a differential pressure $\Delta p$.

oscillations, the compressor will enter surge. Surge is more easily described on the basis of an extended compressor map, see Figure 2.3. The stable operating region of the compressor lies to the right of point B in Figure 2.3, where pressure rise decreases for increasing flow. Also assume that the compressor speed is constant, implying that the operating point lie on the speed line shown in the figure. The surge cycle can then be described by the following steps:

1. Assume that the compressor operates at point A, when the downstream pressure starts to increase. This causes compressor flow to decrease to the point where no further pressure rise through the compressor is possible, marked by B.

2. If the downstream pressure still exceeds the maximum pressure increase, flow will decrease and even become negative at point C. The negative flow causes the upstream pressure to increase, and as a result the pressure rise over the compressor goes down.

3. At point D, the upstream pressure of the compressor is almost equal to the downstream pressure. The compressor will then restore positive flow.

4. Flow will continue to increase until reaching point A. If no means are employed to move out of the surge region, the surge cycle will repeat.

For a variable speed compressor, the stable and unstable regions of operation are separated by the surge line (SL). This line is usually determined by considering the points on the compressor map where the pressure rise increase is zero for increasing flow, which includes point B in 2.3.

The SL is usually independent of the energy efficiency, which is one of the variables defining compressor characteristics. The remaining three variables are coupled through the relations given by the compressor map. Consequently only two variables are needed to describe the SL. But due to the non-linear compressor characteristics, the operating point of the compressor is not uniquely determined by every combination of these two variables, e.g. speed and pressure rise.

The surge phenomenon, unlike rotating stall, is a system instability which affects all states of the compression system. Speaking in terms of control theory, the surge cycle has the characteristics of a limit cycle.

Compressor surge may cause severe damage to the machinery and both upstream and downstream components and is therefore highly undesireable. Various means for preventing the occurance of surge or stabilizing the compressor when operating in the surge region will be presented later.

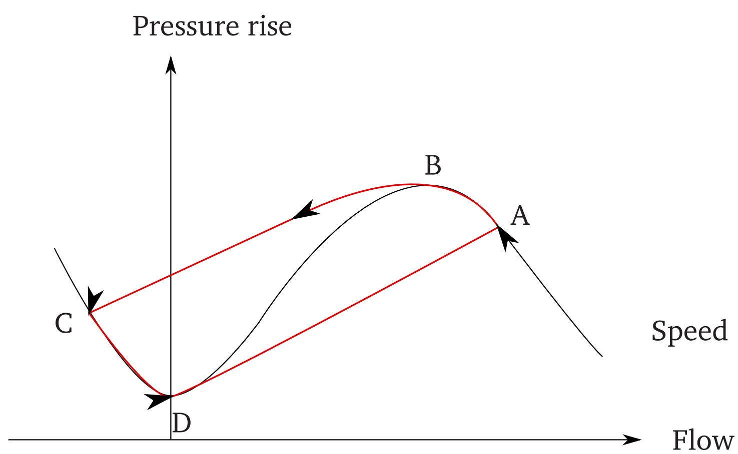


**Figure 2.3:** Illustration of surge, cycle marked by red.

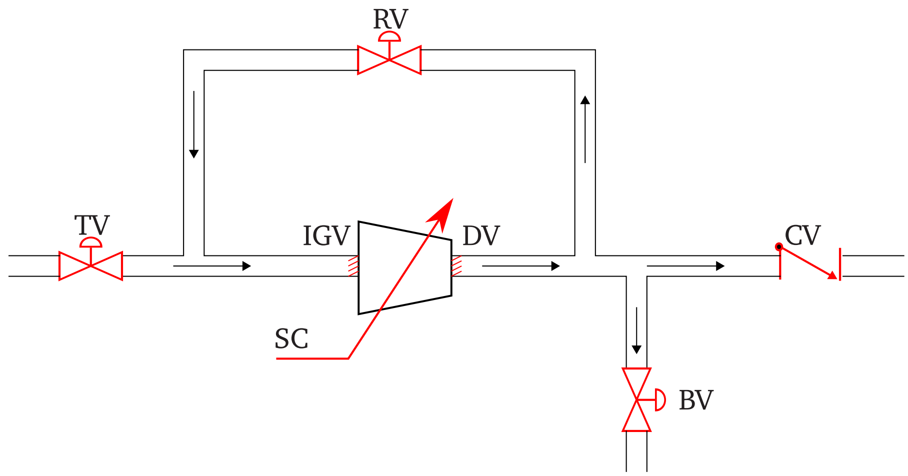


**Figure 2.4:** Compressor control approaches. Control means marked red and arrows indicate fluid flow direction. TV: Throttle valve, RV: Recycle valve, BV: Blow-off valve, CV: Check valve, IGV: Inlet guide vanes, DV: Diffuser vanes, SC: Speed control.

## 2.2 Compressor control

Compressors are naturally designed on the basis of its operating conditions. However, operating conditions will change on both short and long term basis, necessitating the introduction of controllers. When operating a compressor, there are essentially two possibly conflicting control goals: Protection and performance [3]. Protection relates to keeping the compressor from entering damaging conditions, hereunder surge prevention. By performance is meant the act of delivering desired pressure rise and flow while maximizing energy efficiency.

There are several means for compressor control used to reach the control goals. In Figure 2.4, the placement of various approaches relative to the compressor is illustrated. The approaches are not necessarily all present in the same compression system and some also have similar results of actuation.

The throttle valve is mainly used for performance control, ensuring that the flow through the compressor and/or upstream pressure is within the desired limits. The same applies to the inlet guide vanes and diffuser vanes. Adjusting these vanes change the flow versus compression relationship such that a given pressure rise may be accomplished for smaller flows without increasing compressor speed. However, compressor speed controllers are also widely used with similar results, but allowing the speed to change.

Recycle, blow-off and check valves are usually installed with the intention of protecting the compressor against potentially damaging operation. Recycle and blow-off valves will allow greater fluid flow through the compressor than through the total compression system. Fluid that is recycled or blown off represents a waste of energy, as the compressed fluid never reaches the output of the compression system. Check valves are installed such that fluid never is able to flow in the reverse direction. Further, if the check valve closes, pressure downstream of the compressor rapidly decreases if the recycle or blow-off valve opens, such that forward flow is quickly restored. Recycle valves are usually installed where the gas itself is valuable, not only the pressure rise, such as natural gas compression systems. Blow-off valves are used in air compression applications as air can be released directly into the atmosphere.

Even though the preceding means of control have been categorized by their initial reason for installment, they are also able to affect their opposing control goal. Speed control e.g. may be used to aid the recycle valve controller against the destructing effects of surge. Coordinated control have the potential to both increase compressor performance while ensuring safe operation.

### 2.2.1 Surge control

This section presents some of the most important control schemes developed for surge control. The history of compressor surge control spans at least from 1917 [4] to present. This rich past combined with the wide range of compressor applications results in many different control schemes. Even though surge control strategies have evolved from simple mechanical devices to state of the art computer based active surge control, insight in the development of compressor control is of importance. The industry is conservative when considering new technology, especially for safety critical applications. Therefore, relatively old control schemes are still deployed in existing plants.

In general, technology specifications are protected by their owning company, which limits the possibility of obtaining direct knowledge from the developer. However, the same protective behavior results in patents open to the general public. The literature reviewed in this survey is consequently to a large extent based on filed patents. In addition to patents, articles on general compressor dynamics and control are consulted with the aim of increased insight and understanding.

Due to the vast number of patents only a selection of these can be reviewed. The selection represents the main trends and evolution of control schemes. The number of times that a patent has been cited by later patents and patents assigned by main contributors in the field of compressor control, are believed to be of special importance. Existing control strategies can according to [5] and [2] be divided into three groups, characterized by their control goals. The groups are called surge avoidance, surge detection and avoidance, and active surge control.

Surge avoidance has the aim of preventing surge by keeping the operating point away from the surge region. Usually a static or dynamic surge control line related to the surge lin is established, which increases the illegal region of operation. This category is the main focus of this thesis and will be further examined.

Surge detection and avoidance scheme inventors emphasize that some disturbances will cause the compressor operating point to enter the surge region, regardless of avoidance strategy. Further, surge avoidance schemes will effectively decrease the operating range of the compressor reducing its performance. Establishment of the surge line and corresponding surge control line requires detailed knowledge of the compressor's geometry and construction, as well as operational values such as temperature, gas composition and pressure. These challenges are not overcome by monitoring the operating point of the compressor, but by detecting incipient surge. Measurements reflecting characterisics of incipient surge are converted into a surge control variable which is compared to some threshold. When exceeded, means for recovering from the surge condition are initiated. This eliminates the need for calculating the compressor operating point and its distance to the surge line. Examples of patents are found in [6], [7] and [8]. This approach is fundametally different from surge avoidance, where surge is prevented prior to its occurance.

Active surge control is a relatively new discipline of compressor control, according to [2] first introduced in the literature by [9]. The goal of active surge control is to extend the operating range of the compressor into the surge region by suppressing the effects caused by surge. The surge region can be regarded as open loop unstable. By introducing a controller, the compressor can be stabilized also in the unstable region.

### 2.2.2 Surge avoidance with recycle valve

In [5] a comprehensive overview and discussion of different surge control strategies from its start to 1990 is presented. Surge avoidance schemes are grouped into four categories. The categorization is based on how the three variables suitable to describe proximity to surge are combined into a control variable.

- Category one is called “Conventional anti-surge control” and encompass strategies where only flow and differential pressure across the compressor are measured. The control line is usually established by a static relationship between the measurements. The author describes some controller structures. A trend is that the inventions have special means for reacting to rapid disturbances. Also, the controller tuning parameters are not static, but depend on the rate of approach or distance to the control line.

- Category two, “Flow/rotational speed”, the pressure rise of the compressor is neglected. Instead, the fluid flow is normalized by the compressor rotational speed to form a single variable which is compared to a set point.

- Category three, “Microprocessor and PLC [2] Based Controller”, is characterized by including measurements in addition to flow and pressure rise. Variables such as inlet temperature are measured to accurately calculate the operating point and its location in the compressor map.

- Category four, “Control without flow measurements”, avoid the possibly inaccurate and noisy flow measurement when computing the control variable. Pressure rise and compressor rotational speed or torque are the most common measurements.

[2]Programmable Logic Controller.

With the work done by [5] in mind, patents from the time after 1990 have been examined. The focus has been on the proposed controller structure, along with the presented control variable.

In [10] a control scheme addressing the non-linear characteristics of the surge line is proposed. A given change in pressure rise results in different response of the control system determined by placement of the operating point in the compressor map. This is referred to as variable gain. As the control system performance is heavily influenced by the gain, it should be determined by the system designer. The invention provides a system and device for balancing the effects of variable gain, such that the total gain of the system is constant for all operating points. The input to a PID controller is adjusted according to the gradient of the non-linear surge control line at the operating point. A gain scheduling approach is also proposed, by calculating different gains for different operating points in advance. Including a discrete filter for the gain scheduled values removes the discontiunous jumps which exist for gain scheduling. The standard flow rate and pressures upstream and downstream of the compressor are used to form the control variable, placing this invention in category one.

The standard PID controller may not be able to prevent surging if disturbances are fast and/or flow rate is small. In [11], the inventor proposes an additional controller which opens a quick acting solenoid valve when flow rate is below a static threshold. A selector chooses between the the signals from the standard PID controller and the fast response controller. Time dependent functions are used to ensure smooth transitions between the two controllers and provide extra safety margins when the quick emptying valve has been employed.

A similar approach is proposed in [12]. The conventional PID controller is used and the control variable belongs to in chategory one. To be able to withstand fast disturbances, an additional IPID controller is introduced. The control variable of the latter is the rate of change of the conventional PID's control variable. According to the inventor, the additional integrator in the rate controller will cause the system to settle down even if the operating point is outside the active region of the conventional PID controller. To allow higher fluctuations when operating far from the surge region, the setpoint of the rate controller is adjusted correspondingly.

In [13], the rate of approach to the surge line is counteracted by adjusting the surge control line. First, a control variable which includes inlet and outlet temperatures, compression ratio and flow rate, and compressor rotational speed and guide vane position is calculated, a category three approach. Simultaneously, the surge control line is established by adding to the surge line a steady state bias, an adaptive control bias determined from the time derivative of the control variable, and a surge count bias based on the number of surge events experienced. The distance from the control variable to the surge control line is input to a PI controller. The distance is also sent to an open-loop controller, which increments its control output if the distance is below a predetermined threshold. Finally, the outputs from the two controllers are added and the sum determine the anti surge valve opening.

Another dynamic surge control line is applied in [14], on the basis of the category one variables flow rate and pressure rise. It is claimed that in the most common control schemes, the valve is closed when operating to the right of the control line, even if it approaches the surge region rapidly. The invention solves this by introducing a rate dependent bias on the surge control line, calculated by the current distance to the set point substracted by a time delayed signal of the same distance. The time delay is large when the operating point approaches the surge line, and small if it is directed away from the surge line.

An application note for compressor control by a specified controller is given in [15]. The controller itself has a standard PID structure including integral anti-windup. But in addition, the closing rate is limited. This allows the PID controller to be tuned for fast response, while at the same time avoiding that the valve is closed equally fast.

The invention in [16] comprises a control variable that is claimed to be independent of molecular weight of the gas, compressor speed, temperature and/or pressure. This way a single universal surge line can be plotted for all operating conditions, and control is performed only by measuring flow, inlet and outlet pressures, resulting in a category three scheme.

The scheme presented in [17] also pursues a control variable invariant of operating conditions, which especially adresses the the problems encountered when the surge line is nearly horizontal. The basis of the control variable is the one encountered in e.g. [13], but further manipulated into a new control variable.

Apparantly, most of the control schemes for surge avoidance with recycle valves encountered in patent literature, incorporate a conventional PID controller. The contributions made by the patents can be divided into two groups:

- Improving response by adding more control structures
- Altering the control variables and measurements

Control under normal operating conditions is usually performed by the PID controller, whereas the patents belonging to the first group tries to improve response when the system is subjected to rapid disturbances or emergency shutdown events (ESD). The patents in the second group aim to render the control system invariant with respect to certain system variables and/or operating conditions.

## 2.3 Implementation issues

When implementing anti surge control strategies, one has to take into account practical implementation aspects. Some of these aspects will be discussed in the following section, with the aim to justify, describe and clarify existing anti surge strategies.

### 2.3.1 Invariance

Preferably, the operating point of the compressor should be given by variables invariant of the operating conditions of the compressor. Invariant variables describes the distance to the surge limit in a uniform manner suited for anti-surge control. If the compressor map were to be expressed by these invariant variables, it would be fixed for all inlet conditions. An invariant compressor map is naturally only valid for a specific compressor, but this limitation is due to the geometry and construction of the compressor, not its operating conditions. For the discussion of anti-surge control, variables describing energy efficiency are not important. Consequently, variables related to the latter characteristic will not be presented.

Variables regarded invariant are not universal. There exist many different combinations of the physical quantities related to compressor operation which are claimed to be invariant, see e.g. [13] and [16]. In [3], three invariant variables are presented. They are related to the three compressor characteristics eligible to describe the surge line mentioned in Section 2.1.1. The variables are reduced volumetric flow $q_r$, reduced polytropic head $h_r$ and equivalent speed $N_r$ given by:

$$q_r = \frac{q_s}{\sqrt{\frac{Z_s R T_s}{M}}} \tag{2.1}$$

$$h_r = \frac{R_p^{\sigma} - 1}{\sigma} \tag{2.2}$$

$$N_r = \frac{N}{\sqrt{\frac{Z_s R T_s}{M}}} \tag{2.3}$$

Subscript $d, s$ denote variables measured at compressor outlet and inlet respectively. The symbols $Z, T$ represent compressibility [3] and temperature, $q$ is volumetric flow, $R_p = p_d/p_s$ pressure ratio, $R$ is the universal gas constant, $M$ is the molecular mass of the gas and $\sigma$ is the exponent for polytropic compression. The increase in energy through the compressor is assumed to be a polytropic process [4], and in most applications this implies that $\sigma$ can be assumed constant.

If inlet temperature and gas composition can be assumed constant, other simpler and more intuitive variables can be used. The variables $q_r$, $h_r$ and $N_r$

[3] The compressibility $Z \leq 1$ is an empirically based correction factor describing how close a gas behaves to an ideal gas. For an ideal gas $Z = 1$ [3].

[4] A polytropic process is a thermodynamic process where the relationship $pV^n$ is constant, $p$ is pressure, $V$ is volume and $n$ is the constant polytropic index [3].

are then invertible functions [5] of $q$, $R_p$ and $N$ respectively. Consequently, the latter variables may be assumed to be invariant.

For the remaining of this thesis, the volumetric flow on the SL is given as a function of pressure ratio:

$$q_{SL} = j(R_{p,SL}) \tag{2.4}$$

Even though the control variable should be invariant to varying inlet conditions, compressor maps are rarely given in terms of the previously presented invariant variables. Non-invariant compressor maps are only valid for given reference operating conditions. However, because the compressor map, or more specifically surge line, is the basis for developement of compressor control strategies, non-invariant variables should be corrected to fit the reference conditions. This correction is performed via the invariant variables.

If flow is represented by mass flow $w$, a correction factor can be found by considering flow at different conditions, relating them to volumetric flow and inserting ideal gas law (2.12):

$$\begin{aligned}
\frac{w_m}{\rho_m} &= q = \frac{w_r}{\rho_r} \\
\frac{RT_m}{p_m M} w_m &= \frac{RT_{ref}}{Mp_{ref}} w_r \\
w_r &= \frac{T_m/T_{ref}}{p_m/p_{ref}} w_m
\end{aligned} \tag{2.5}$$

Measured and corrected values are subscripted $m$ and $r$ respectively, while $ref$ denote the reference condition given in the compressor map. For simplicity, it is assumed that the gas composition is equal to its reference, such that the gas molar mass $M$ can be eliminated.

Similarly to volumetric flow corrections, measured differential pressure $\Delta p_m = p_d - p_s$ over the compressor should be adjusted to fit the differential pressure $\Delta p_c$ for reference inlet pressure used in the compressor map. By assuming that the compression ratio $R_p = p_d/p_s$ is invariant of inlet conditions, the measured differential pressure should be corrected according to:

$$\begin{aligned}
\frac{p_r}{p_{ref}} &= \frac{p_d}{p_s} \\
\Delta p_r &= p_r - p_{ref} \\
&= (\frac{p_d}{p_s} - 1)p_{ref} \\
&= \Delta p_m \frac{p_{ref}}{p_s}
\end{aligned} \tag{2.6}$$

### 2.3.2 Surge control line

The compression system stability does not only depend on the compressor, but also its surroundings. Nevertheless, the SL is used for synthesis of the anti-surge

[5] An invertible function describes a one to one relationship between the function argument and function value in some domain, [18].

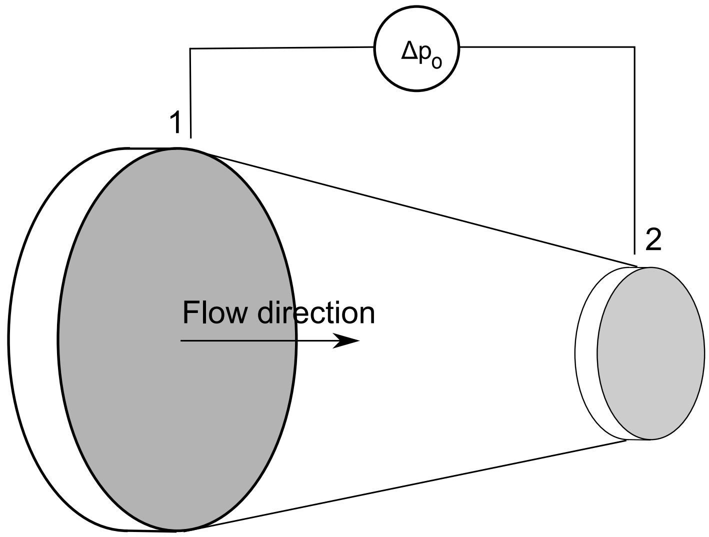


**Figure 2.5:** Fluid flow through orifice.

control strategy, or more specifically the surge control line (SCL) given by:

$$q_{SCL} = c(R_{p,SCL}) \tag{2.7}$$

The SCL is usually constructed by adding a static or dynamic safety margin to the SL. Both the SL and SCL describe the system charateristics in steady state conditions. However, when the SCL line is employed in a controller, measurements of the pressure ratio $R_p$ are used as an input to (2.7). Measured flow is compared to this value giving an estimate of the operating point's proximity to SCL. From this, two general observations are made. First, the SL/SCL describes the compressor operation in steady state conditions, whereas non-steady state pressure ratio is used as an input to the SCL. Second, the proximity of the operating point to the surge line does not necessarily represent the shortest distance from the operating point to the SCL. These aspects will be further examined later.

### 2.3.3 Flow measurement

Anti-surge controllers usually require measurement of mass or volumetric flow through the compressor. The principles of measuring flow may comprise temperature, electromagnetism or pressure [19], where the latter is most widely used.

Flow measurement through differential pressure readings can be illustrated by examining fluid flow through a pipe orifice, see Figure 2.5. At the points marked $1, 2$, the cross sectional areas $A_1, A_2$ are known. The differential pressure $\Delta p_o = p_1 - p_2$ is measured. However, the results are also valid for other differential pressure flow measurement devices based on the Bernoulli equation such as Pitot tubes. The Bernoulli equation is developed for incompressible and inviscid fluids [6] [20], essentially expressing conservation of energy for fluids. Assuming horizontal flow, the equation takes the form:

$$\frac{p_1}{\rho} + \frac{v_1^2}{2} = \frac{p_2}{\rho} + \frac{v_2^2}{2} \tag{2.8}$$

where $v_1, v_2$ are flow velocities in point $1$ and $2$. The mass flow $w$ is equal through the cross sections, assuming no mass accumulation. The pipe and orifice hole are assumed to have circular cross sections with diameters $d_1, d_2$:

$$w = \rho A_1 v_1 = \rho A_2 v_2 \tag{2.9}$$

Combining (2.8) and (2.9), solving for mass flow, gives:

$$\begin{aligned} w &= c_d \sqrt{\frac{2\rho\Delta p_o}{\frac{1}{A_2^2} - \frac{1}{A_1^2}}} \\ &= c_d A_2 \sqrt{\frac{2\rho\Delta p_o}{1-\gamma^4}} \\ &= c_f A_2 \sqrt{2\rho\Delta p_o} \end{aligned} \tag{2.10}$$

where $c_d$ is a coefficient included to correct for frictional losses and other measurement errors introduced by the geometry of the orifice, and $\gamma$ is the ratio of orifice hole to pipe diameter $d_2/d_1 < 1$.

### Gas expansion factor

The preceding result is based on the assumption that compression effects are negligible for the differential pressure between points $1, 2$. For gases, compression effects may be included by multiplying (2.10) with the gas expansion factor:

$$Y = \sqrt{R_o^{2/k}\left(\frac{k}{k-1}\right)\left(\frac{1-R_o^{(k-1)/k}}{1-R_o}\right)\left(\frac{1-\gamma^4}{1-\gamma^4 R_o^{2/k}}\right)} \tag{2.11}$$

where $R_o = \frac{p_2}{p_1}$ and $k = \frac{c_p}{c_v}$ is the specific heat ratio. For derivation of this factor, see [20].

Usually, the differential pressure is small compared to the static pressure of the gas, and the gas expansion factor can be omitted or included as a constant. This is justified by comparing the ratio of non-corrected versus corrected flow for measurement ranges in a real plant. The results are presented in Figure 2.6, where both orifice differential pressures $\Delta p_o$ and static pressure $p_1$ is altered. The measurement errors are below 2.5 percent which is assumed to be sufficient for control purposes. Hence, the gas expansion factor will not be included in the further analysis.

[6] Incompressible fluids do not change density when compressed, inviscid fluids essentially does not experience friction forces [20].

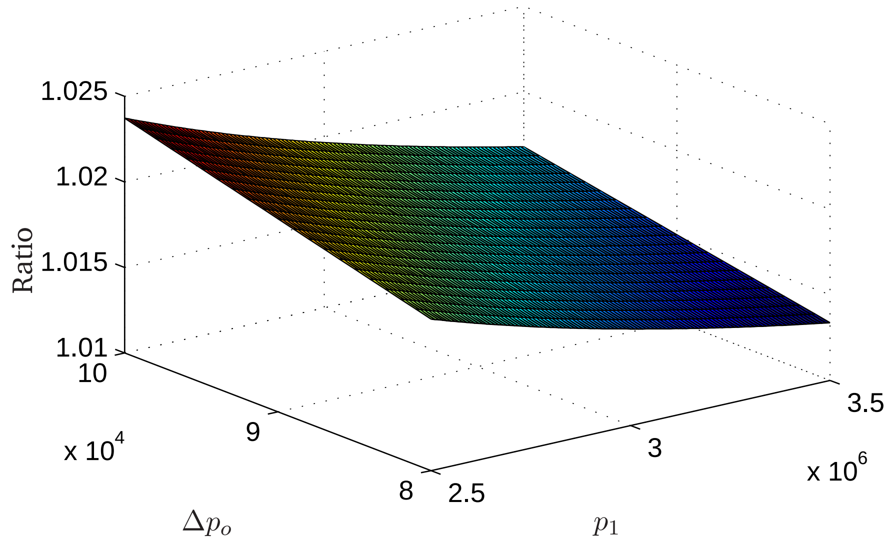


**Figure 2.6:** Non-corrected versus corrected mass flow ratio.

### Density variations

However, the assumption of incompressible fluid is not generally valid for gases. The density of the gas will vary with the static pressure, and consequently this effect should also be compensated for. The ideal gas law states that:

$$p = \rho \frac{R}{M} T \tag{2.12}$$

where $R$ is the universal gas constant, $M$ is the molar mass of the gas and $T$ is gas temperature as previously defined. Replacing $\rho$ in (2.10) and assuming constant temperature and gas composition gives:

$$w = c_f A_2 \sqrt{2 p_1 \frac{M}{RT} \Delta p_o} = c_w \sqrt{p_1 \Delta p_o} \tag{2.13}$$

where $c_w = c_f A_2 \sqrt{\frac{2M}{RT}}$.

Volumetric flow can be computed from mass flow and orifice differential pressure according to:

$$q = \frac{w}{\rho} = c_{qw} \frac{w}{p_1} = c_q \sqrt{\frac{\Delta p_o}{p_1}} \tag{2.14}$$

where $c_q = c_f A_2 \sqrt{\frac{2RT}{M}}$ and $c_{qw} = \frac{c_q}{c_w} = \frac{RT}{M}$.

In Figure 2.7, the density correction as a function of pressure is illustrated. Mass flow is computed with and without density corrections for the same pressure ranges used in Figure 2.6. The ratio of these mass flows is given on the y-axis. It is recognized that the errors introduced by assuming constant density are significantly larger than by those caused by not including the gas expansion factor.

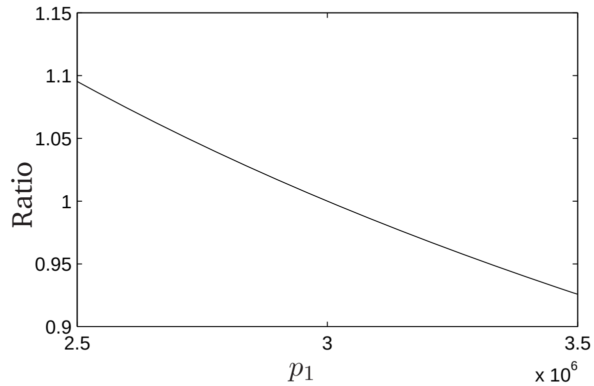


**Figure 2.7:** Non-corrected versus corrected mass flow ratio.

### 2.3.4 Pressure measurements

Pressure measurements are not nearly as complicated as flow measurements. Many principles of pressure measurements exist, each with different error sources and dynamic behaviour [19]. However, the error sources are not as closely related to the system states as for flow measurements. For simplicity, pressure measurements are assumed to be perfect in the remaining of this thesis.

### 2.3.5 Control valve characteristics

Flow in the compression system is usually controlled by inserting valves in pipes and ducts. The steady state flow through a valve can be modeled by [21, page 35]:

$$w_v = C_v^*(l)\sqrt{2\rho\Delta p} \tag{2.15}$$

where $w_v$ is the mass flow through the valve, $C_v^*(l)$ is the valve flow coefficient, $l \in [0,1]$ is the valve opening, $\rho$ is the upstream density of the fluid and $\Delta p = p_1 - p_2$ is the pressure drop across the valve.

The flow coefficient $C_v^*$ is calculated in steady state conditions, at a certain opening position and where $\Delta p = 1Pa$. The term valve characteristics is used to describe how the flow coefficient varies as a function of opening position. There are three common valve characteristics:

- Linear $C_v^* = C_{v,max}^* l$.
- Quick opening $C_v^* = C_{v,max}^* l^{1/\mu}, \quad \mu > 1$.
- Equal percentage $C_v^* = C_{v,max}^* \phi^{l-1}, \quad \phi \approx 50$

Valves with linear and equal percentage characteristics are mainly used for control purposes, whereas quick opening valves are ideal for applications where large flow rates should be delivered as quickly as possible.

The recycle valve opening is regulated by a positioner, whose set point is given by the anti-surge controller. Consequently, the resulting recycle flow from a commanded valve opening will vary depending on the valve characteristics.

As previously presented, anti-surge strategies are often based on standard linear PI(D) controllers with constant gains. However, the linear structure of the PID controller will be distorted if employing valves with non linear characteristics. This may complicate controller tuning, as the valve response will be highly dependent on its opening.

# Chapter 3

# Modeling

The mathematical model used for analysis is based on the compression system with recycle valve model presented in [22, page 504], which again is based on the famous Greitzer surge model from 1976. The model captures the main characteristics related to surge expressed by a set of differential equations. Previously discussed phenomena apart from surge encountered in a compression system, e.g. rotating stall, are not covered by the model. However, as the inherent goal of the anti surge controller is avoiding surge, other phenomena are of limited interest. The model is developed by considering three principal models; pressure dynamics in a control volume, duct flow dynamics and shaft dynamics. The models presented will not be derived from their fundamental origin, for further insight the reader is adviced to consult e.g. [22] and other references.

## 3.1 Pressure dynamics

A gas compression system inludes a considerable amount of piping where fluid is able to accumulate. Further, in many gas compression systems the wet and dry parts of a fluid is separated in a component called a scrubber, ensuring that no liquid enter the compressor. However, two phase flow [1] is out of scope of this thesis. By assuming that the amount of liquid accumulated in the scrubber is constant, the size of the volume occupied by gas will also be constant.

The presented pressure dynamic model may also be used to represent interconnecting ducts, such that duct flow can be regarded one dimensional.

The pressure dynamics are derived by regarding a fixed control volume with uniform density. The rate of change of mass in the volume is described by:

$$V\dot{\rho} = w_{in} - w_{out} \tag{3.1}$$

$V$ is the control volume size, $\rho$ is the density of the gas, $w_{in}, w_{out}$ are the mass flows in and out of the volume. The relationship may be further refined by assuming that the gas in the volume is ideal, see Equation (2.12), and that the

[1] Two phase flow contain both liquids and gases [23].

thermodynamic behaviour of the gas can be regarded isentropic [2]:

$$dp = c_i^2 d\rho \tag{3.2}$$

where $c_i$ is the sonic velocity in the volume. The pressure differential equation for a volume is then finally given by:

$$\dot{p} = \frac{c_i^2}{V}(w_{in} - w_{out}) \tag{3.3}$$

## 3.2 Duct flow

Compression systems include, as mentioned, pipes or ducts in which fluid flows between system components. The duct fluid flow also represent dynamic relationships suitable to be expressed by differential equations. Flow can be modeled by considering the momentum equation of the fluid inside of the duct. The duct is assumed to have constant cross sectional area $A$ and connects two volumes with pressures $p_1$ and $p_2$. Further, fluid is assumed incompressible, one dimensional and with uniform axissymmetric velocity. The momentum equation for the duct is then given by:

$$\frac{d}{dt}(mv) = Ap_1 - Ap_2 + F' \tag{3.4}$$

where $m = LA\rho$ is the total fluid mass in the duct, $v = \frac{w}{\rho A}$ is the fluid velocity, and $F'$ describes the sum of all internal forces in the duct. $L$ reflects the actual fluid flow path length which does not necessarily correspond to the physical length of the duct.

Rewriting (3.4) gives a differential equation for the duct mass flow:

$$\dot{w} = \frac{A}{L}(p_1 - p_2 + F) \tag{3.5}$$

where $F = \frac{1}{A}F'$.

## 3.3 Shaft dynamics

Centrifugal compressors are large rotating systems, and the dynamics of the shaft will also affect the total compression system. The compressor may be actuated by different drives. However, the drive dynamics are not in the scope of this thesis, hence drive torque is assumed to be delivered instantly. Shaft dynamics are modeled from conventional torque balance:

$$\dot{\omega} = \frac{1}{J}(\tau_u - \tau_l) \tag{3.6}$$

where $\omega$ is the rotational speed of the compressor, $J$ is the inertia of all rotating parts in the compressor, $\tau_u$ is the drive torque, and $\tau_l$ is the load torque.

[2] A isentropic process resemble a polytropic process where $pV^n$ is constant, and no heat is removed from or added to the gas [3].

The drive torque is assumed to be controlled by a conventional PID controller, whose aim is to keep the shaft rotational speed constant at $\omega_d$. The PID controller is given by:

$$\tau_u = K_p e_\omega + K_d \dot{e_\omega} + K_i \int e \quad dt \tag{3.7}$$

$$e_\omega = \omega_d - \omega \tag{3.8}$$

The controller output is dependent on precise measurement of rotational speed. This measurement is assumed to be perfect, hence the rotational speed $\omega$ will be directly used in the drive torque PID controller.

A simple load torque model is found in [22, page 488]. By assuming radial vanes in the impeller, the load torque is given by:

$$\tau_l = r^2 w_c \omega \tag{3.9}$$

where $r$ is the radius at the impeller outlet and $w_c$ is the compressor mass flow.

### Error dynamics

To include the PID controller in the total compression system dynamics, the error dynamics of the shaft and speed controller is derived. Differentiating (3.8) with respect to time, and inserting (3.6), (3.7) and (3.9) gives:

$$\begin{aligned} \dot{e_\omega} &= -\dot{\omega} = -\frac{1}{J}(K_p e_\omega + K_d \dot{e_\omega} + K_i \int e_\omega dt - r^2 w_c(\omega_d - e_\omega)) \\ &= -\frac{1}{K_d + J}(K_p e_\omega + K_i \int e_\omega dt - r^2 w_c(\omega_d - e_\omega)) \\ \ddot{e_\omega} &= -\frac{1}{K_d + J}((K_p + r^2 w_c)\dot{e_\omega} + K_i e_\omega - r^2 \dot{w}_c(\omega_d - e_\omega)) \end{aligned} \tag{3.10}$$

## 3.4 Compressor characteristics

Compressor modeling is traditionally based on empirical studies of compressors in steady state, which result in the previously described compressor map. The compressor map can also be derived by considering an isentropic process in series with an isobaric process, for details consult [22]. In any case, the resulting compressor characteristics must be related to the duct flow dynamics from (3.5). First, assume that the compressor characteristic is given by:

$$\frac{p_d}{p_s} = \Psi_c(q_c, \omega) \tag{3.11}$$

where $p_d, p_s$ are pressures at the outlet and inlet of the compressor, and $\Psi_c : \mathbb{R}\mathbf{x}\mathbb{R} \rightarrow \mathbb{R}$ is the compressor map giving the pressure ratio of the compressor as a function of volumetric flow $q_c$ through the compressor and rotational speed $\omega$ of the compressor shaft. The mapping from volumetric flow and rotational speed to pressure ratio implies that internal flow dynamics inside the compressor are fast compared to the overall compression system.

The duct mass flow (3.5) is in steady state condition given by:

$$p_1 - p_2 = \Delta p = -F \tag{3.12}$$

In steady state, the pressure at the compressor inlet equals the pressure in the upstream volume, and the compressor outlet pressure equals the downstream volume pressure. Consequently, the compressor characteristic is related to the general duct flow force by:

$$F = \Psi_c(q_c, \omega)p_1 - p_1$$

which inserted into (3.5) gives:

$$\dot{w}_c = \frac{A_c}{L_c}(\Psi_c(q_c, \omega)p_1 - p_2) \tag{3.13}$$

representing the mass flow through the compressor in term of volume pressures upstream and downstream and the compressor map. The mass flow $w_c$ and volumetric flow $q_c$ are related, however the two notations are preserved to illustrate that the compressor map is expressed by invariant coordinates discussed in Section 2.3.1.

## 3.5 Valve flow

The flow dynamics for ducts where valves are inserted are derived similarly to the compressor flow, on basis of the equations given by (3.5) and (2.15).

By inserting the ideal gas law (2.12) into (2.15), the steady state flow can be expressed for different upstream pressures:

$$w_r = C_r(l)\sqrt{p_1 \Delta p} \tag{3.14}$$

where $C_r(l) = C_v^*(l)\sqrt{2\frac{M}{RT}}$. Further, combining (3.14) and (3.12), gives:

$$F = -\frac{1}{p_1 C_r(l)^2}|w_r|w_r \tag{3.15}$$

Finally, the dynamic behaviour of mass flow through the recycle line is given by:

$$\dot{w}_r = \frac{A_d}{L_d}(p_1 - p_2 - \frac{1}{p_1 C_r(l)^2}|w_r|w_r) \tag{3.16}$$

To avoid division by zero, $l$ in $C_r(l)$ is set to be in the range $l \in [\epsilon_l, 1], \quad 0 < \epsilon_l << 1$. This implies that a small leakage flow through the valve occurs even when fully closed. However, this implication will also be encountered in real applications where the differential pressure over the valve is high [21].

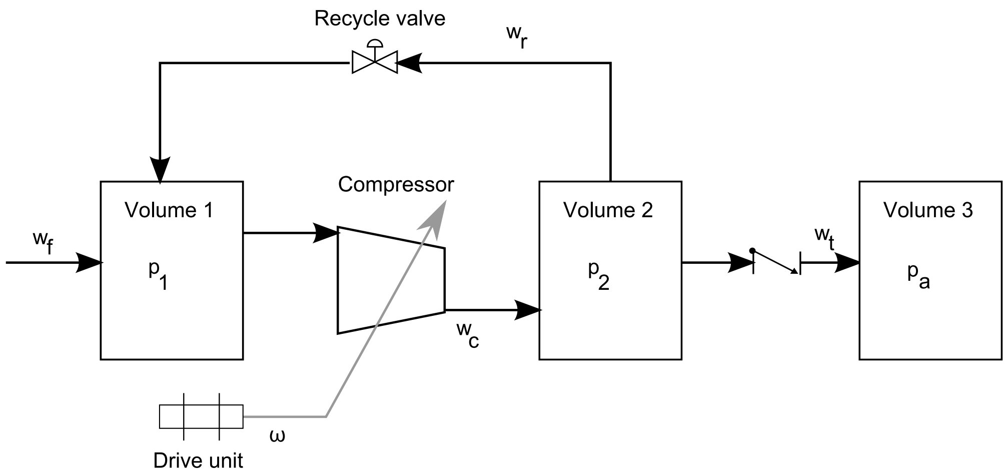


**Figure 3.1:** Compression system with recycle line.

### 3.5.1 Check valve flow

Check valves only allow flow in one direction preventing reversed flow into the system. The ideal check valve has zero pressure loss, implying that $F = 0$ from (3.5). Consequently, the mass flow through the check valve is given by:

$$
\begin{aligned}
\dot{w}_t &= \frac{A_t}{L_t}(p_1 - p_2) \\
w_t &> 0
\end{aligned}
\tag{3.17}
$$

## 3.6 Compression system model

The preceding component models are assembled into a complete model for the compression system with recycle line, see 3.1. Pressure dynamics in the volumes 1 and 2 denoted $p_1, p_2$ respectively, are described by (3.3). Volume 1 represents the scrubber and piping upstream of the compressor, while volume 2 is a relatively small volume downstream of the compressor inserted in the intersection of the compressor duct and the recycle line. Volume 3 is assumed to be so large that $p_a$ is constant.

Flow through the compressor $w_c$ is given by (3.13). The inlet and outlet pressures of the duct where the compressor is mounted is given by the pressure in volume 1 and volume 2, respectively.

Further, recycle line flow $w_r$ is given by (3.16) where it is assumed that pressure drop over the recycle valve equals pressure difference in volume 1 and 2.

Check valve flow $w_t$ is governed by (3.17), whereas feed flow $w_f$ is considered a system disturbance.

Finally, the compressor shaft dynamics are incorporated through the corresponding error dynamics from (3.8).

The total compression system model is then given by:

$$\begin{aligned}
\dot{p_1} &= \frac{c_1^2}{V_1}(w_f - w_c + w_r) \\
\dot{p_2} &= \frac{c_2^2}{V_2}(w_c - w_r - w_t) \\
\dot{w}_c &= \frac{A_c}{L_c}(\Psi_c(c_{qw}\frac{w_c}{p_1}, \omega)p_1 - p_2) \\
\dot{w}_r &= \frac{A_r}{L_r}(p_2 - p_1 - \frac{1}{p_2 C_r(l_r)^2}|w_r|w_r) \\
\dot{w}_t &= \frac{A_t}{L_t}(p_2 - p_a) \\
\ddot{e_\omega} &= -\frac{1}{K_d + J}((K_p + r^2 w_c)\dot{e_\omega} + K_i e_\omega - r^2\frac{A}{L_c}(\Psi_c(w_c, \omega)p_1 - p_2)(\omega_d - e_\omega))
\end{aligned} \tag{3.18}$$

The measurements in the system are given by the measurement vector $y$:

$$y = \begin{bmatrix} p_1 \\ p_2 \\ \Delta p_o \end{bmatrix} = \begin{bmatrix} p_1 \\ p_2 \\ \frac{w_c^2}{c_w^2 p_1} \end{bmatrix} \tag{3.19}$$

The pressures of volumes 1 and 2 are assumed to be measured directly, whereas the flow through the compressor is measured by a flow element. The relationship between differential pressure across a flow element and mass flow is presented in (2.13). Measurement of shaft rotational speed is not included in $y$, as this is implicit in the speed error dynamics.

## 3.7 Comments

The model (3.18) does not include temperature dynamics. In many gas compression systems, temperature is regulated by heat exchangers to ensure high energy efficiency in the compressor. Consequently, inlet temperature is assumed to be constant, density computed from ideal gas law Equation (2.12) is a function of pressure only. This assumption can be justified by examining the ratio of temperature measurements versus the mean temperature value, and the ratio of inlet pressure measurements versus the mean pressure value. Measurements are taken from a real plant, and the ratios are presented Figure 3.2. It is recognized that pressure varies considerably more than temperature, hence density changes are mainly caused by pressure dynamics.

The temperature regulation violates the assumption of an isentropic process used in the derivation of the volume 1 pressure dynamics, as heat is removed from the system. However, recycle flow will partly compensate for the heat loss as the temperature of fluid on the compressor outlet usually is higher than the temperature at the inlet.

The small volume 2 downstream of compressor may not meet the assumptions regarding uniform density when check valve is closed. Inflow and outflow

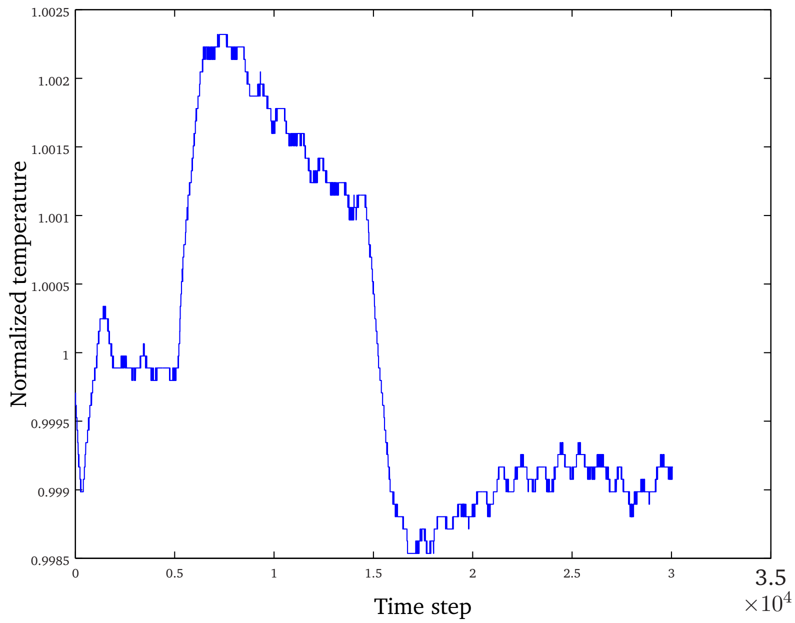


**Figure 3.2:** Changes in temperature versus changes in pressure.

regions of the volume where fluid velocity is non zero will affect density, and the size of these regions are significant compared to the total volume. However, for positive throttle flow, volume 2 may be regarded as an integral part of large volume 3. Hence, the model is more accurate when regarding positive throttle flow.

Regarding the recycle valve operation, no assumptions about the valve characteristics have been made. Hence, the system input $u$ covers a wider range of possible implementations. The size of $u$ will still be limited by the minimum and maximum values of the valve opening given by the assumptions for (3.15).

## 3.8 State space representation framework

The model (3.18) and strategies are transformed into a uniform state space framework for further analysis. The scope of this thesis lie on the different anti surge control strategies. Consequently, the compressor speed is assumed to be perfectly controlled and the error dynamics are neglected:

$$
\begin{aligned}
\dot{x} &= f(x) + g(x)\frac{1}{u} + e(x)v \\
y &= h(x) \\
z &= i(y)
\end{aligned}
\tag{3.20}
$$

where $x$ denotes the system state space vector, $u$ the scalar system input, $v$ is disturbance vector, $y$ is the measurement vector, $z$ the scalar control variable and $f, g, e, h, i$ are vector functions. Finally, the system constants are gathered in a vector $a$. The scalars, vectors and functions are defined by:

$$\begin{aligned} x &= \begin{bmatrix} p_1 & p_2 & w_c & w_r & w_t \end{bmatrix}^T \\ u &= C_r(l_r)^2 \\ v &= \begin{bmatrix} w_f & p_a \end{bmatrix}^T \\ a &= \begin{bmatrix} \frac{c_1^2}{V_1} & \frac{c_2^2}{V_2} & \frac{A_c}{L_c} & \frac{A_r}{L_r} & \frac{A_t}{L_t} & \frac{1}{c_w^2} & c_{qw} \end{bmatrix}^T \end{aligned} \tag{3.21}$$

$$\begin{aligned} f(x,u,a,v) &= \begin{bmatrix} a_1(-x_3+x_4) \\ a_2(x_3-x_4-x_5) \\ a_3(\psi_c(\frac{x_3}{x_1})x_1-x_2) \\ a_4(x_2-x_1) \\ a_5x_2 \end{bmatrix} \\ g(x) &= \begin{bmatrix} 0 & 0 & 0 & -a_4\frac{|x_4|x_4}{x_2} & 0 \end{bmatrix}^T \\ e(x) &= \begin{bmatrix} e_1 & e_2 \end{bmatrix} = \begin{bmatrix} a_1 & 0 & 0 & 0 & 0 \\ 0 & 0 & 0 & 0 & -a_5 \end{bmatrix}^T \\ h(x) &= \begin{bmatrix} x_1 & x_2 & a_6\frac{x_3^2}{x_1} \end{bmatrix}^T \end{aligned} \tag{3.22}$$

The function $i(y)$ differ for the different anti surge control strategies, and is treated in later sections. Note also that the compressor map is represented by $\psi_c(\frac{x_3}{x_1})$, assuming that the compressor speed is constant for the given timeframe.

## 3.9 Equilibrium

The equilibrium of the system when the recycle line is closed is determined by its boundary conditions or disturbances. The SCL can be viewed as a manifold separating the unactuated and actuated regions of compressor operation. If the disturbances imply that the equilibria of the unactuated system lies to the left of the SCL, the recycle valve must be opened to ensure safe operation of the compressor. Assuming that the anti surge controller is able to drive the control variable to zero, the actuated system will have its equilibria on the SCL. This can be stated as:

$$c(R_{p,e}) = q_e \tag{3.23}$$

where $c(\cdot)$ is the function from (2.7), and subscript $e$ denotes the equilibrium. The shaft rotational speed of the compressor is assumed controlled. If the speed controller regulates speed according to a predetermined set point value $\omega_d$, the equilibrium of the actuated compression system will be explicitly determined by the intersection of the corresponding speed line in the compressor map and the SCL, see Figure 3.3.

The equilibrium for the whole compression recycle system can be found from (3.20), setting all derivatives to zero and assuming that the recycle valve must

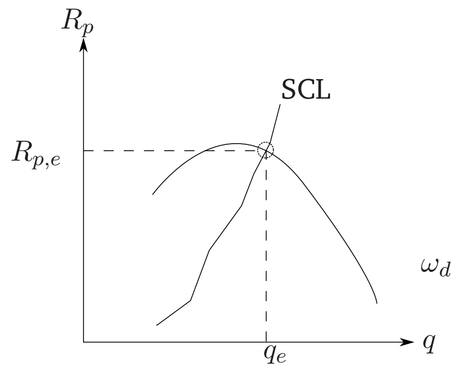


**Figure 3.3:** Equilibrium of actuated system.

be actuated to remain on the SCL by introducing the relationship from (3.23):

$$\begin{aligned} x_{1e} &= \frac{v_2}{R_{p,e}} \\ x_{2e} &= v_2 \\ x_{3e} &= \frac{v_2 q_e}{a_7 R_{p,e}} \\ x_{4e} &= \frac{v_2 q_e}{a_7 R_{p,e}} - v_1 \\ x_{5e} &= v_1 \\ u_e &= \frac{(\frac{v_2 q_e}{a_7 R_{p,e}} - v_1)^2}{v_2^2(1 - 1/R_{p,e})} \end{aligned} \tag{3.24}$$

The presented equilibria are valid for positive values of recycle flow, or:

$$\frac{c(R_{p,e})}{R_{p,e}} > \frac{a_7 v_1}{v_2} \tag{3.25}$$

which limits possible pressure ratio equilibria from below.

### System input equilibrium

The equilibrium of the system input is dependent on the compression ratio where the SCL is defined. However, the latter observation does not imply that the largest system input on the surge line is given by the highest compression ratio. This can be explored by regarding the derivative of the equilibrium $u_e$ with respect to compression ratio $R_{p,e}$. If negative, this means that an increase in compressor speed will in fact require the recycle valve to be closed to remain on the SCL. Further, if the derivative equals zero:

$$\frac{\partial u_e}{\partial R_{p,e}} = 0$$

will after some calculation imply that:

$$\frac{c(R_{p,e})}{R_{p,e}} - \frac{a_7 v_1}{v_2} = 0 \tag{3.26}$$

or

$$c(R_{p,e})(2 - \frac{1}{R_{p,e}}) + 2c'(R_{p,e})(1 - R_{p,e}) - \frac{a_7 v_1}{v_2} = 0 \tag{3.27}$$

where $c'(R_{p,e}) = \frac{\partial c}{\partial R_p}|_{R_p = R_{p,e}}$. The relationship in (3.26) describes the equilibrium with zero recycle flow which does not comply with the criterion from (3.25). However, if (3.27) is satisfied for a compression ratio in the compressor's region of operation, the minimum and maximum valve openings will not necessarily appear at the extremal values of compressor speed.

This previous aspects seem surprising, as an increase in speed means that more fluid should pass through the compressor to stay on the SCL. Assuming unchanged disturbances, the compressor flow increase must be a result of increased flow through the recycle line. However, the differential pressure across the recycle valve will also be risen due to the speed change, such that the required flow is achieved without further opening the recycle valve.

***Example 3.1***

Assume that the SCL is given by:

$$c(R_p) = c_0 \sqrt{R_p - 1}$$

Inserted into (3.26), will after some algebraic manipulation give:

$$R_{p,e}^3 - (3 + (\frac{a_7 v_1}{v_2 c_0})^2) R_{p,e}^2 + 3R_{p,e} - 1 = 0 \tag{3.28}$$

whose solutions are determined by the slope of the SCL and the size of the disturbances. The existence of solutions for positive values of $R_{p,e}$ can be examined by using the Descartes' sign rule [24]. The rule states that the maxium number of negative zeros for a polynomial $P(x)$ can be found from counting the number of sign changes in $P(-x)$. Applied to (3.28), it is recognized that zero sign changes occurs. Consequently, all solutions of (3.28) are positive, showing that peaks in system input equilibrium may be encountered for feasible compression ratios.

# Chapter 4

# Analysis

This chapter first presents tools to categorize and analyse different anti surge strategies and characteristics concerning the model (3.20), followed by a section where the tools are applied on presented strategies. Finally, simulations emphasizing strategy characteristics are shown.

## 4.1 Strategy analysis

The different anti surge strategies will be assessed by their invariance according to those discussed in in 2.3.1. However, the strategies also differs in the structure of the control variable and SCL. Some general properties of the dynamics of the control variable when seen in relation to the whole compression system will also be presented.

### 4.1.1 Surge control line

The SCL is constructed by adding a safety margin to the SL. An expression for the this way of constructing the SCL is given by:

$$c(R_{p,SCL},t) = b_1(R_{p,SL},t)j(R_{p,SL}) + b_0(R_{p,SL},t) \tag{4.1}$$

where $b_1$ alters the slope of the SL, and $b_0$ give an offset to the SL, see Figure 4.1. Time varying SCL parameters are presented in e.g. [14] and [13] aiming to dampen fast disturbances and avoid recurring surge events. The SCL may also be specified by a smooth function, e.g.:

$$c(R_{p,SCL}) = c_0\sqrt{R_{p,SCL} - 1} \tag{4.2}$$

where it is ensured that the SCL lies to the right of the surge line for the whole operating region of the compressor.

### 4.1.2 Control variable structure

The control variable $z$ describes the relation between a set point value $\bar{q}_d(c(R_p))$ generated from the SCL and measured value $\bar{q}(q)$ generated from flow. Depending on the sign of controller gains, $z$ is positive or negative whenever $\bar{q}_d > \bar{q}$. In the remaining of this thesis $z > 0$ if $\bar{q}_d > \bar{q}$.

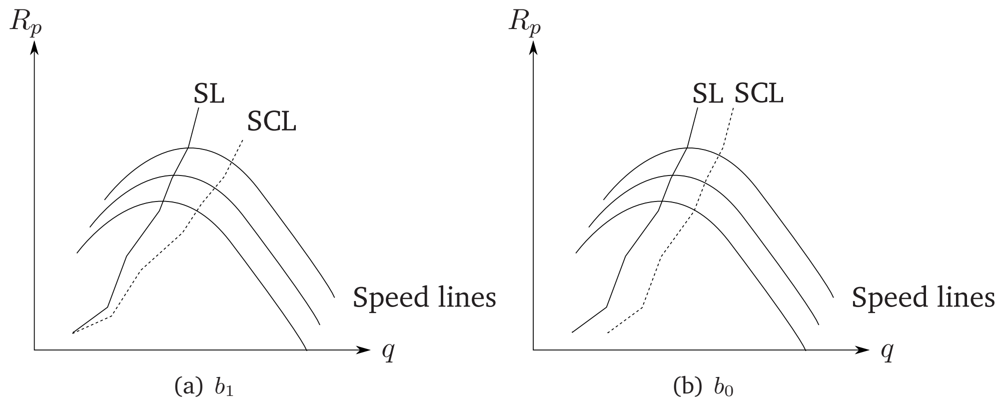


**Figure 4.1:** Effect of SCL parameters.

There are many ways to satisfy the latter criterion. Due to the linear structure of the PID controller, the traditional synthesis of the variable $z$ is a linear combination of $\bar{q}_d, \bar{q}$ given by:

$$z_1 = \bar{q}_d - \bar{q} \tag{4.3}$$

Another structure used in the industry is given by:

$$z_2 = 1 - \frac{\bar{q}}{\bar{q}_d} \tag{4.4}$$

This normalization scheme cancels out terms which are common for both $\bar{q}_d$ and $\bar{q}$. However, it also implies that deviations from setpoint are expressed relative to the set point value. This can be clarified by relating the two schemes according to:

$$z_1 = z_2 \bar{q}_d \tag{4.5}$$

Assuming that (4.4) determines the control variable, insertion of (4.5) into a general expression for a PID controller gives:

$$u = \frac{K_p}{\bar{q}_d} z_1 + K_d \frac{d}{dt}(\frac{z1}{\bar{q}_d}) + K_i \int \frac{z_1}{\bar{q}_d} \quad dt \tag{4.6}$$

The behaviour of this choice of control variable is not as transparent as the choice of (4.3). If assuming a constant set point $\bar{q}_d$, it is clear that the controller gains are determined by the size of the set point.

***Example 4.1***

To illustrate the various aspects concerning the control variable and SCL, a simple example is presented. Assume that control variable is given by :

$$z = c(R_p)^2 - q^2$$

according to the structure in (4.3), and the SCL according to (4.2):

$$c(R_p) = c_0 \sqrt{R_p - 1} \tag{4.7}$$

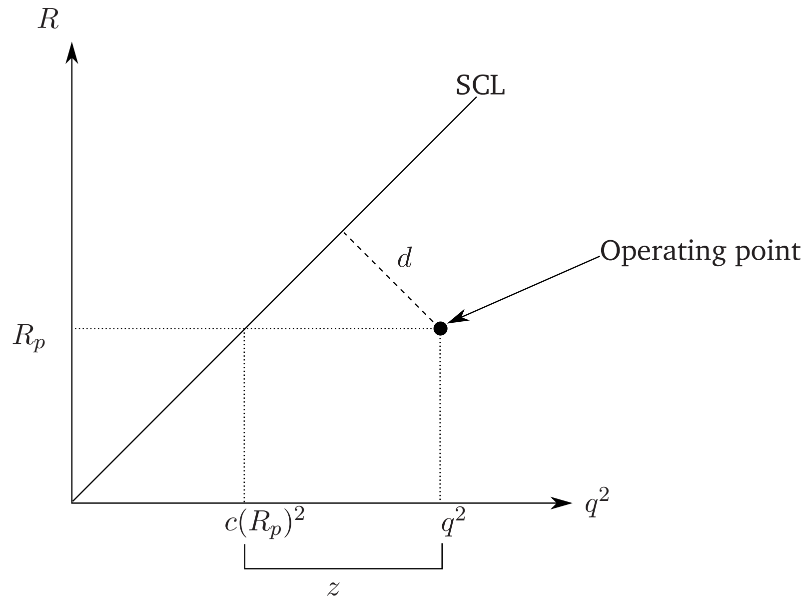


**Figure 4.2:** Shortest distance.

This choice of $z$ always gives the shortest distance $d$ between the operating point and the SCL in terms of:

$$d = z\frac{1}{\sqrt{c_0^2 + 1/c_0^2}}$$

A geometric interpretation of this result is found in Figure 4.2. However, another choice of SCL structure would lead to a shortest distance which is not explicitly given by the control variable.

The preceding example illustrates a general problem by representing the proximity of the operating point to SCL in a scalar variable. This distance may be calculated parallel to the flow axis, the pressure rise axis, as the shortest distance from the operating point to the SCL etc. In [17], it is claimed that a linear or non-linear combination of invariant coordinates is also invariant. Consequently, the SCL may be given in terms of combinations of invariant parameters, hereafter called $m_a$ and $m_b$. If the relationship between $m_a$ and $m_b$ on the SCL is linear, the shortest distance from the operating point to SCL can be represented by a control variable computed on the $m_a$ or $m_b$ axis. In the example, $m_a = R$ and $m_b = q^2$, and the control variable gives a distance parallel to the $m_b$ axis.

### 4.1.3 Control variable dynamics

As the measurements are known functions of the state space variables and the control variable is given by these measurements, the control variable as a function of state space variables is given by:

$$z = i(h(x)) \triangleq k(x) \tag{4.8}$$

The time derivative of the control variable is:

$$\begin{aligned}
\dot{z} &= \frac{\partial k(x)}{\partial x}\dot{x} \\
&= \frac{\partial k(x)}{\partial x}(f(x) + g(x)\frac{1}{u} + e_1 v_1 + e_2 v_2) \\
&= L_f k(x) + L_g k(x)\frac{1}{u} + L_{e_1} k(x) v_1 + L_{e_2} k(x) v_2 \\
&= L_f k(x) + L_{e_1} k(x) v_1
\end{aligned} \tag{4.9}$$

where $L_f k(x) = \frac{\partial k(x)}{x} f(x)$ is called the Lie derivative of k with respect to f. It is recognized that the term $L_g k(x) = 0$, which means that the first time derivative of the control variable is independent of system input u. This is clarified by rewriting $L_g k(x)$:

$$\begin{aligned}
L_g k(x) &= \frac{\partial k(x)}{\partial x} g(x) \\
&= \frac{\partial i(h(x))}{\partial x} g(x) \\
&= \frac{\partial i(y)}{\partial y}\frac{\partial h(x))}{\partial x} g(x)
\end{aligned} \tag{4.10}$$

where:

$$\frac{\partial h(x))}{\partial x} g(x) = \frac{\partial h(x_1, x_2, x_3))}{\partial x}\begin{bmatrix} 0 & 0 & 0 & -a_4 \frac{|x_4| x_4}{x_2} & 0 \end{bmatrix}^T \qquad = 0$$

The measurements are only dependent on states $x_1, x_2, x_3$ while the system input appears in the differential equation describing $\dot{x_4}$. This is independent of the choice of control variable, as long as the current measurements are utilized. The same applies to $L_{e_2} k(x)$.

The second time derivative of the control variable is, assuming constant disturbances:

$$\begin{aligned}
\ddot{z} &= \frac{\partial [L_f k(x) + L_{e_1} k(x) v_1]}{\partial x}\dot{x} \\
&\quad + \frac{\partial [L_f k(x) + L_{e_1} k(x) v_1]}{\partial x}\dot{v} \\
&= L_f^2 k(x) + L_g L_f k(x)\frac{1}{u} + L_{e_1} L_f k(x) v_1 + L_{e_2} L_f k(x) v_2 \\
&\quad + L_f L_{e_1} k(x) v_1 + L_g L_{e_1} k(x) v_1 \frac{1}{u} + L_{e_1}^2 k(x) v_1^2 + L_{e_2} L_{e_1} k(x) v_1 v_2 \\
&\triangleq m(x, u, v)
\end{aligned} \tag{4.11}$$

### Linearization

The system presented in (3.20), can be studied for small pertubations around an equilibrium through linearization [25, page 99]. The linearized system is given by:

$$\begin{aligned}
\Delta \dot{x} &= A\Delta x + B\Delta u + E\Delta v \\
\Delta z &= C\Delta x
\end{aligned} \tag{4.12}$$

where

$$
\begin{aligned}
A &\triangleq \frac{\partial(f(x)+g(x)\frac{1}{u}+e(x)v)}{\partial x}|_e \\
B &\triangleq \frac{\partial(g(x)\frac{1}{u})}{\partial u}|_e \\
E &\triangleq e(x)|_e \\
C &\triangleq \frac{\partial(k(x))}{\partial x} \\
\Delta x &\triangleq x - x_e \\
\Delta u &\triangleq u - u_e \\
\Delta v &\triangleq v - v_e
\end{aligned}
$$

The term $|_e$ denotes that the function is evaluated at the equilibrium given by (3.24). Matrices are given in appendix B.

One characteristic of a linear system, is that the frequency response from input change to output change is independent of its operating point. This can be shown by considering a general linear system:

$$
\begin{aligned}
\dot{x^*} &= A^* x + B^* u^* + E^* v^* \\
z^* &= C^* x^*
\end{aligned}
$$

The linear system equilibrium is given by:

$$
\begin{aligned}
x_e^* &= (A^*)^{-1}\left[B^* u_e^* + E^* v_e^*\right] \\
z_e^* &= C^* x_e^*
\end{aligned}
$$

Hence, when the linear system dynamics are expressed by deviations from the equilibrium, we get:

$$
\begin{aligned}
\Delta \dot{x^*} &= A^* \Delta x^* + B^* \Delta u^* + E^* \Delta v^* \\
\Delta z^* &= C^* \Delta x^*
\end{aligned}
$$

The transfer functions are given by:

$$
H_u^*(s) = \frac{N_u^*(s)}{D_u^*(s)} = C^*\left(sI - A^*\right)^{-1} B^* \tag{4.13}
$$

$$
H_v^*(s) = \frac{N_v^*(s)}{D_v^*(s)} = C^*\left(sI - A^*\right)^{-1} E^* \tag{4.14}
$$

Consequently, the transfer functions (4.13) and (4.14) from control variable and disturbances, respectively, are independent of the operating point of the system.

This is not generally valid for a linearized system, as the matrices $A, B, C, E$ are dependent on the equilibrium. However, a non-linear system's linearity may be examined by regarding the transfer function of the linearized system in different equilibria. Specifically, by calculating the eigenvalues and zeroes of the linearized system, the main governing dynamics may be identified. How these eigenvalues and zeroes are affected by changes in equilibrium, will give insight in the behaviour of the system in different equilibria. Further, for small frequencies the steady state gains given by $H_u(0)$ and $H_v(0)$ can be used to determine how the system gain is affected by equilibrium changes.

Applied to the compression system, the equilibria of interest lie on the SCL. As previously mentioned, operating conditions which require an open recycle valve to ensure safe operation of the compressor, give a system equilibrium on the SCL. The SCL is parameterized in terms of the compression ratio $R_{p,e}$, but one should bear in mind that that an increase in steady state compression ratio corresponds to increasing the compressor speed.

The size of the steady state gain is not interesting by itself, as the steady state deviation caused by slow varying disturbances will be cancelled by the integral effect in a controller. But for the purpose of controller tuning, it is necessary to determine the area where the input to output gain is larger. If the input-output gain increases significantly, a PID-controller with constant controller gains have to be tuned such that the closed loop stability for high compression ratios is maintained. However, a large gain difference might imply that the response to a disturbance for low compression ratios is insufficient to avoid surge. On the other hand, if the input-output gain increase is small, the response to a disturbance for low compression ratios may be excessive such that oscillations are induced.

## 4.2 Strategy 1

Control of the compression system is made on the basis of measured compressor pressure rise $\Delta p_c = p_2 - p_1$ and differential pressure over an orifice $\Delta p_{o,m}$.

### 4.2.1 Invariance

The differential pressure over the orifice representing compressor flow and inlet pressure are combined according to:

$$\bar{q} = \Delta p_{o,m} \frac{K_f}{p_1} = \frac{q_c^2 K_f}{c_q^2} \tag{4.15}$$

where $K_f$ is an adjustment constant. Hence, the flow variable is proportional to volumetric flow squared. As volumetric flow is regarded as an invariant variable, the same applies to the given flow variable. For simplicity, the relationship $K_f/c_q^2 = 1$ is used in the further analysis.

The differential pressure over the compressor is divided by inlet pressure giving:

$$\frac{\Delta p}{p_1} = R_p - 1 \tag{4.16}$$

As previously discussed, pressure ratio can be regarded as an invariant variable. Consequently, the proposed pressure rise parameter is also invariant.

### 4.2.2 Surge control line

The surge control line is computed from the surge line by adding a margin in percentage of flow, or:

$$c(R_{p,SCL}) = 1 + b_1 j(R_{p,SL}) \tag{4.17}$$

$$\bar{q_d} = c(R_p)^2 \tag{4.18}$$

### 4.2.3 Control variable structure

The control variable is computed from difference between $\bar{q_d}$ and $\bar{q}$ in correspondance with (4.3):

$$z = c(R_p)^2 - q_c^2 \tag{4.19}$$

The control variable can also be described by introducing the relation from (3.23), and describing the compressor flow in terms of volumetric flow $q_c$:

$$\begin{aligned} z &= c(R_p)^2 - q_c^2 \\ &= c(R_p)^2 - c(R_{p,e})^2 + q_e^2 - q_c^2 \qquad (4.20) \\ &= (c(R_p) - c(R_{p,e}))(c(R_p) + c(R_{p,e})) + (q_e - q_c)(q_e + q_c) \\ &= \Delta c(R_p)(\Delta c(R_p) + 2c(R_{p,e})) + \Delta q_c(2q_e - \Delta q_c) \\ &= 2q_e(\Delta c(R_p) + \Delta q_c) + \Delta c(R_p)^2 - \Delta q_c^2 \qquad (4.21) \end{aligned}$$

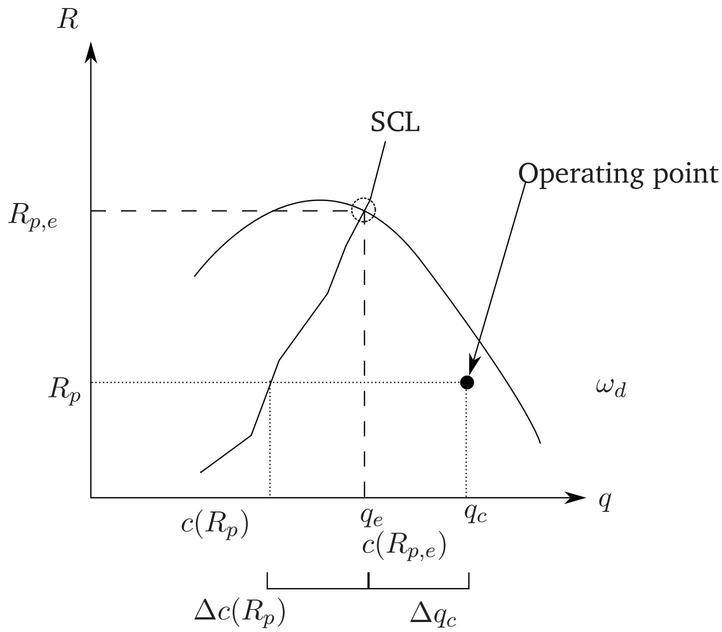


**Figure 4.3:** Interpretation of control variable.

where $\Delta c(R_p) = c(R_p) - c(R_{p,e})$ and $\Delta q_c = q_e - q_c$. Hence, the control variable is the sum of distances from equilibrium in volumetric flow and pressure ratio tranformed through the SCL, in addition to two terms of squared distances, see Figure 4.3.

For constant linear deviations from the SCL, $c(R_p) - q_c = k_0$, which describes operating points on a line parallel to the SCL, the control variable is given by:

$$\begin{aligned} z &= c(R_p)^2 - q_c^2 \\ &= (c(R_p) - q_c)(c(R_p) + q_c) \\ &= k_0(k_0 + 2q_c) \\ &= k_0^2 + 2k_0 q_c \end{aligned} \tag{4.22}$$

To the left of the SCL, $k_0 > 0$. Consequently, the size of the control variable for a given deviation increases for increasing volumetric flow through the compressor. However, as discussed in section 4.1.2, a linear deviation does not necessarily represent the shortest distance to the SCL.

***Example 4.1***

If the SCL is given by (4.2), the control variable from (4.20) is equal to:

$$\begin{aligned} z &= c_0(R_p - 1) - c_0(R_{p,e} - 1) + q_e^2 - q_c^2 \\ &= c_0(R_p - R_{p,e}) + q_e^2 - q_c^2 \end{aligned}$$

Adjusting the slope of the SCL by altering the value of $c_0$, corresponds to altering the weighing of the distance from the compression ratio to its equilibrium versus the distance of the compressor flow to its equilibrium.

### 4.2.4 Control variable dynamics

Adapted to the framework from (3.20), (4.19) is given by:

$$\begin{aligned} z = i(y) &= c(\frac{y_2}{y_1})^2 - K_f \frac{y_3}{y_1} \\ &= c(\frac{x_2}{x_1})^2 - a_7 \frac{x_3^2}{x_1^2} \\ &= k(x) \end{aligned} \tag{4.23}$$

The compression ratio $R_p = x_2/x_1$ and the volumetric flow $q_c = a_7 x_3/x_1$ are coupled through the differential equations given in (3.20). We have:

$$\begin{aligned} \dot{q}_c &= a_7 \left( \frac{\dot{x_3}}{x_1} - \frac{x_3 \dot{x_1}}{x_1^2} \right) \\ &= a_7 \left( \frac{\dot{x_3}}{x_1} - q_c \frac{\dot{x_1}}{a_7 x_1} \right) \\ &= a_7 \left( \frac{\dot{x_3}}{x_1} + q_c^2 \frac{a_1}{a_7^2} - q_c \frac{a_1}{a_7}(v_1/x_1 - x_4/x_1) \right), \end{aligned} \tag{4.24}$$

$$\frac{x_2}{x_1} = \psi_c(\frac{q_c}{a_7}) - \frac{\dot{x_3}}{a_3 x_1} \tag{4.25}$$

Inserting the relationships from (4.24) and (4.25) into (4.23), leads to:

$$z = c\Big(\psi_c(\frac{q_c}{a_7}) - \frac{1}{a_3 a_7}\dot{q}_c + \frac{a_1}{a_3 a_7^2} q_c^2 - \frac{a_1}{a_3 a_7}(v_1/x_1 - x_4/x_1) q_c \Big)^2 - q_c^2 \tag{4.26}$$

This means that the control variable is dependent on volumetric flow and its derivative. Used as an input to a PID-controller, it introduces damping effects even if the derivative term of the controller is set to zero. Thus, even when the operating point of the compressor is to the right of the SCL, the valve will be actuated for large fluctuations in flow. Numerous patents, e.q. [12], [13] and [14], has its main focus of improving response to high rates of approach to the SCL. It is pointed out that valve actuation when the operating point is to the right of the SCL, is undesireable. However, the definition of a SCL and using pressure ratio measurements as its input, will implicitly include derivative action.

***Example 4.2***

The compressor map can be approximated in the vicinity of the equilibrium by a first order Taylor series expansion:

$$\begin{aligned} \psi_c(\frac{q_c}{a_7}) &\approx \psi_c(\frac{q_e}{a_7}) + \frac{1}{a_7}(q_c - q_e)\psi_c'(\frac{q_e}{a_7}) \\ &= R_{p,e} + \frac{1}{a_7}(q_c - q_e)\psi_c'(\frac{q_e}{a_7}) \end{aligned}$$

where $\psi_c'(\frac{q_e}{a_7}) = \frac{\partial \psi_c(\frac{q_c}{a_7})}{\partial (q_c/a_7)}|_{q_c = q_e} < 0$. Further, assume that the SCL is given by (4.7).

Inserted into (4.26), and introducing the relationship from (3.23), gives:

$$\begin{aligned}
z &= c_0^2\Big(R_{p,e} + \frac{1}{a_7}(q_c - q_e)\psi_c'(\frac{q_e}{a_7}) - \frac{1}{a_3 a_7}\dot{q}_c + \frac{a_1}{a_3 a_7^2}q_c^2 - \frac{a_1}{a_3 a_7}(v_1/x_1 - x_4/x_1)q_c - 1\Big) \\
&\quad - q_c^2 + q_e^2 - c_0^2(R_{p,e} - 1) \\
&= -\frac{c_0^2}{a_7}\psi_c'(\frac{q_e}{a_7})(q_e - q_c) - \frac{c_0^2}{a_3 a_7}\dot{q}_c - (1 - \frac{c_0^2 a_1}{a_3 a_7^2})q_c^2 + q_e^2 - \frac{c_0^2 a_1}{a_3 a_7}(v_1/x_1 - x_4/x_1)q_c \\
&\approx \frac{c_0^2}{a_7}\psi_c'(\frac{q_e}{a_7})(q_c - q_e) - \frac{c_0^2}{a_3 a_7}\dot{q}_c + q_e^2 - q_c^2
\end{aligned}$$

where the terms $v_1/x_1$, $x_4/x_1$ and $\frac{c_0^2 a_1}{a_3 a_7^2}$ are neglectable due to the physical layout of the compression system and its operating conditions. It recognized that the control variable is given by the deviation between the volumetric compressor flow and the equilibrium point and the time derivative of the same flow. In other words, the difference between the SCL and flow variable, corresponds to a the flow variable's distance to its equilibrium in addition to a damping effect.

### Derivative

The second time derivative of the control variable is found from (4.11) and (4.23):

$$\begin{aligned}
m(x,u,v) = L_f^2 k(x) + L_g L_f k(x) u + [L_{e_1} L_f k(x) + L_f L_{e_1} k(x)]v_1 + L_{e_2} L_f k(x) v_2 \\
+ {L_{e_1}}^2 k(x) v_1^2 \qquad (4.27)
\end{aligned}$$

It can be recognized that $L_g L_f k(x) \neq 0$. According to a term from [26, page 510], the control variable $z$ is said to have relative degree two with respect to the system input $u$.

### Transfer function

The transfer function $H_u(s)$ is given in Appendix C. Even though there are a large number of terms, some conclusions about the system can be made. It is seen that:

$$deg(N_u(s)) = 3 \qquad (4.28)$$

$$deg(D_u(s)) = 5 \qquad (4.29)$$

The linearized system has relative degree $deg(D_u(s)) - deg(N_u(s)) = 2$, which corresponds to the observation from (4.27). Further, as the degree of the denominator of the tranfer function equals the number of system states, there are no pole-zero cancellations for all equilibria on the SCL induced by the choice of strategy. According to [27, page 189], this implies that the system is observable and controllable, and there are no dynamic effects in the system which are not visible through the control varible. However, there may be points on the SCL where the mentioned characteristics are not preserved.

The expression for steady state gain of the compression system $H_u(0) = \frac{N_u(0)}{D_u(0)}$ is given by:

$$N_u(0) = -2{a_7}^2{v_2}^2c\left(R_{p,e}\right){R_{p,e}}^2\left(R_{p,e}-1\right)^2\left(a_7 - \psi_c'(\frac{q_e}{a_7})c'(R_{p,e})\right) \quad (4.30)$$

$$D_u(0) = \left(v_2c\left(R_{p,e}\right) - v_1a_7R_{p,e}\right)\left[\psi_c'\left(\frac{q_e}{a_7}\right)\left(v_2c\left(R_{p,e}\right) - 2v_2R_{p,e}c\left(R_{p,e}\right) + v_1a_7R_{p,e}\right) + 2a_7v_2R_{p,e}(R_{p,e}-1)\right] \quad (4.31)$$

The negative sign illustrates that the control variable decreases when the recycle valve opening increases. The steady state gain size is of limited interest, however attention should be given to the its variations in different equilibria.

Due to the complexity of transfer function, insight is better acquired by regarding a numerical example. The numerical values of the compression system are presented in Appendix A.

### Zeroes and poles

The relative positions of the zeroes and poles of the system in the complex plane is sketched in Figure 4.4. It includes references to Figure 4.5 where the movement of the poles and zeroes for increasing $R_{p,e}$ is illustrated. The system has three distinct poles and one complex conjugate pole pair, one distinct zero and one pair of complex conjugate zeroes. All poles and zeros lie in the left half of the complex plane, except the complex conjugate zero pair. Hence, the system is open loop stable and minimum phase. The transfer function can described in terms of its zeroes and poles:

$$H_u(s) = K\frac{(s+\alpha_5)(s-\alpha_6+\beta_6 i)(s-\alpha_6-\beta_6 i)}{(s+\alpha_1)(s+\alpha_2)(s+\alpha_3)(s+\alpha_3+\beta_3 i)(s+\alpha_3+\beta_3 i)(s+\alpha_4)} \quad (4.32)$$

where $K$ is the transfer function gain, and $\alpha$,$\beta$ denote the real and imaginary parts of the zeroes and poles, respectively. In the following, the zeroes and poles are referenced by their subscript number.

First it is recognized that the pole $1$, $2$ and zero $5$ shown in Figure 4.5(a) are significantly larger in absolute value than the other poles and zeros, hence that parts of the system dynamics are much faster than others. By closer inspection, the size of pole $1$ is found to be assosiated with the size of the system parameter $a_3$, which is related to the compressor duct dimensions. Increasing compressor duct length give slower response. The same arguments may be applied to pole $2$ and system parameter $a_4$. Increasing recycle duct length will move pole $2$ to the right giving slower response. Depending on application and physical layout of the compression system, some or all of these dynamics may very well be neglected, only employing their steady state solutions.

The complex conjugate pole pair denoted $3$ lies to the right of pole $2$ shown in Figure 4.5(b). A complex conjugate pole pair implies that there exist a resonance frequency for the valve opening where the system output will oscillate heavily. Unlike the previously mentioned poles and zeros, the pair moves right

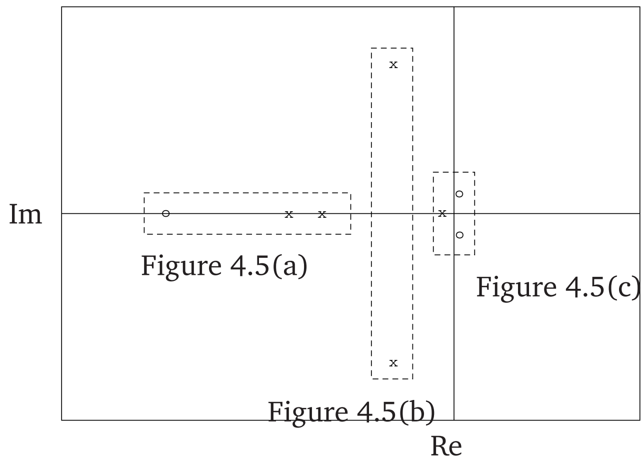


**Figure 4.4:** Relative placement of zeroes and poles, poles marked by crosses and zeroes by circles.

for increasing pressure ratios/speed, such that a speed increase give less damping and more rapid oscillations. Pole pair $3$ is assosiated with parameter $a_5$, causing the resonance frequency to be reduced if check valve duct length is increased.

To the right of pole pair $3$ in the complex plane, lies pole $4$. In absolute value, this is the smallest of all poles and zeros. Consequently, the governing system dynamics are associated to pole $4$. By increasing the value of volume 1, parameter $a_1$ decreases, which again causes pole $4$ to move to the right.

The complex conjugate zero pair $6$ lies in the right half plane with a small real part, hence the linearized system is non minimum phase. In other words, slow opening of the recycle valve will move the control variable to negative values, but fast valve opening may cause the control variable to increase or oscillate even if the system states do not. According to [25], a non minimum phase system is harder to control because of the increased phase lag.

Due to the small real parts of pair $3$ and $6$ compared to their comples values, the exponential behaviour of these dynamics are slow due to the lack of damping. It is also recognized that the imaginary part of these pairs increase for increasing speeds, causing more oscillations for higher speeds.

All poles move strictly to the left when speed is increased, except pole pair $3$ which moves to the right. However, there are no crossing from left to right half plane encountered in the numerical trials. Hence, most of the system dynamics are faster when the compressor speed is increased and stability properties are maintained.

### Frequency analysis

To illustrate the effects caused by the poles and zeros in the previous section, three dimensional bode plot of the transfer function is presented in Figure 4.6. For low frequencies, the system phase is $180^\circ$ due to the negative relationship between the system input and output, where an increase in valve opening causes the control variable to decrease.

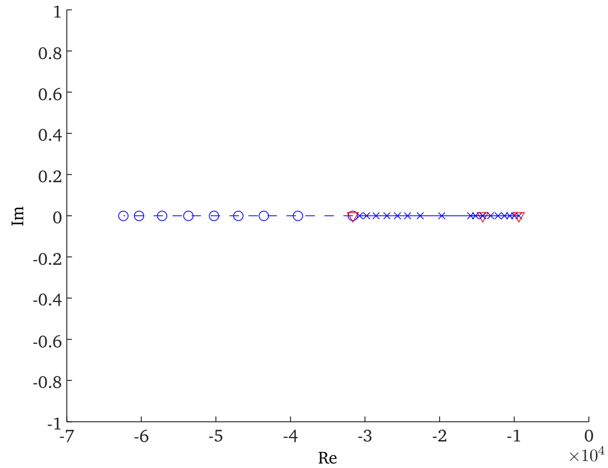


(a) 1,2,5

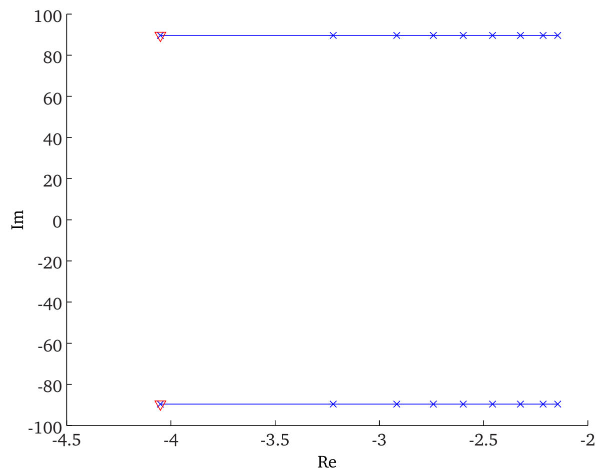


(b) 3

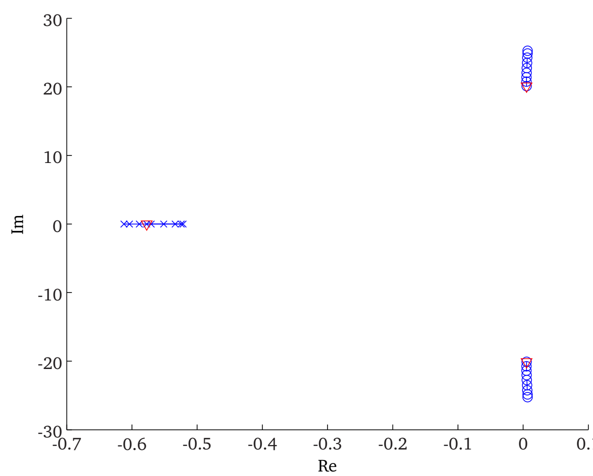


(c) 4,6

**Figure 4.5:** Movement of zeroes and poles, corresponding value for lowest $R_{p,e}$ marked by a red downward pointing triangle.

The pole $4$ is responsible for the drop in phase and amplitude around frequency $1-2\,rad/s$. The amplitude decrease is asymptotically 20dB per decade as expected. The phase also goes down $90\,^{\circ}$.

The first pole is immediately followed by a "'inverse"' resonance frequency caused by the complex conjugate zero $6$ at around $22\,rad/s$. This further decrease the amplitude by 40dB per decade. The phase change because of zero pair $6$ is negative by $180\,^{\circ}$, illustrating the non minimum phase property of the system.

The resonance frequency caused by pole pair $3$ appears around $90\,rad/s$, with the effect of further decreased phase and a peak in amplitude. By actuating the valve at this frequency, heavy oscillations may be induced in the system.

The last shown impact on the amplitude and phase diagrams is seen at around $1000\,rad/s$, caused by pole $2$. The zero $5$ and pole $1$ appear for frequencies significantly higher than those visualized in Figure 4.6.

By vizualizing the bode diagrams for increasing speeds, it has been shown that the qualitative behaviour for increasing speeds is conserved. The differences manifest as altered frequency where amplitude and phase changes occur.

#### Steady state gain

Figure 4.7 shows the steady state gain from system input to control variable for increasing compressor speed, which corresponds to an increase in $R_{p,e}$. The gain is normalized by its lowest value to illustrate the relative gain change in different equilibria. It is recognized that the gain increases for increasing compressor speed/pressure ratio, and the highest value is about 3.6 times larger than the smallest.

This result is independent on the choice of valve characteristics, as the response of the control variable for a small change in valve opening does not depend the initial size of the valve opening. Consequently, if the control variable from this strategy is used as input to a PID-based anti surge controller, tuning should be performed at the highest possible compressor speed to ensure that closed loop system stability is maintained.

The lines in Figure 4.8 show the change in steady state gain from the disturbances $v_1, v_2$ to control variable or $H_v(0)$, which corresponds to feed flow and volume 3 pressure respectively. The gains show a similar behaviour, increasing for increasing compressor speed. However, the gain increase is not as large as from system input. If a rapid disturbance occur in the high speed area, the control variable will react more vigorously than in the low speed area.

## 4.3 Strategy 2

The measurements utilized in the control strategy are $\Delta p_{o,m}$ and $\Delta p_m$, representing flow and pressure rise over the compressor respectively.

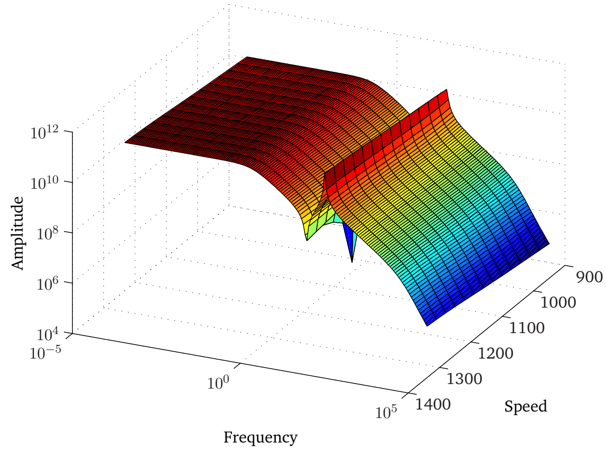


(a) Amplitude

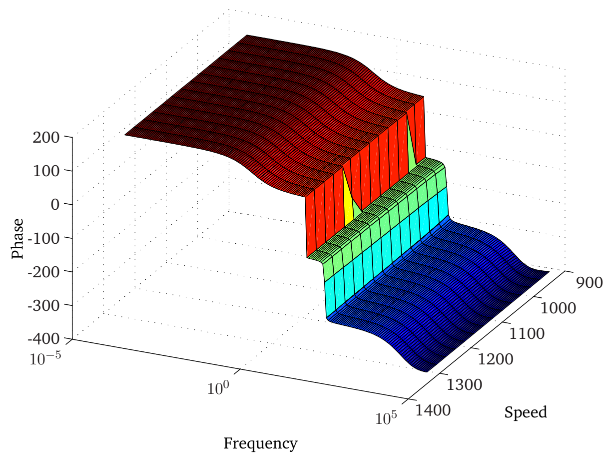


(b) Phase

**Figure 4.6:** 3D bode plot.

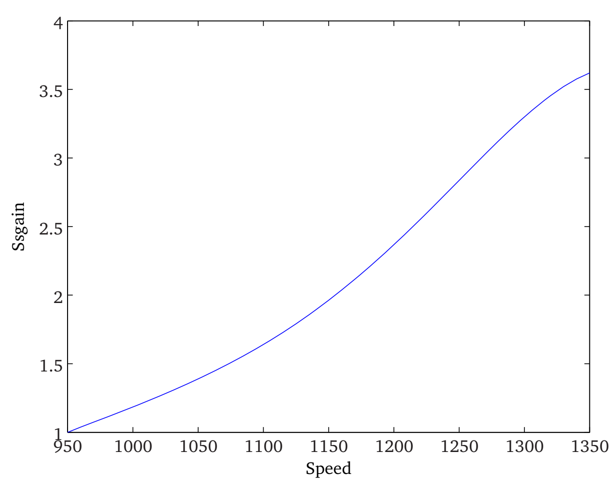


**Figure 4.7:** Normalized steady state gain for system input over a range of compressor speeds.

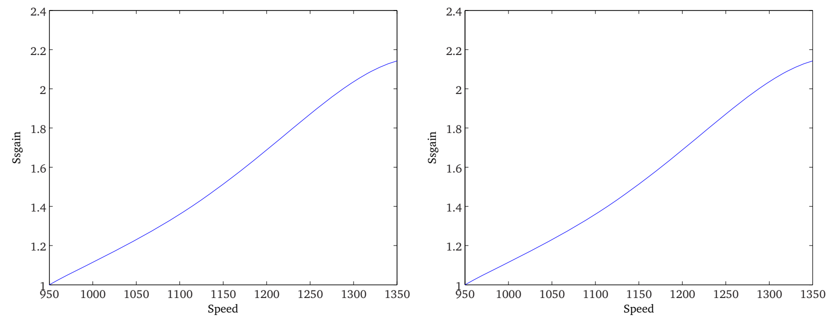


(a) $v_1$ (b) $v_2$

**Figure 4.8:** Normalized steady state gain for disturbances.

### 4.3.1 Invariance

The orifice differential pressure measurement is transformed into a flow variable $\bar{q}$ according to:

$$\bar{q} = \Delta p_{o,m} \frac{p_{ref}}{p_1} = \frac{q_c^2 p_{ref}}{c_q^2} \tag{4.33}$$

$$\tag{4.34}$$

Hence, the flow variable is proportional to volumetric flow squared. As volumetric flow is regarded as an invariant parameter, the same applies to the given flow variable. For simplicity, the relationship $p_{ref}/c_q^2 = 1$ is used in the further analysis.

The pressure rise through the compressor is corrected by the relationship:

$$\Delta p_n = \Delta p_m \frac{p_{ref}}{p_1} \tag{4.35}$$

This is similar to the correction presented in (2.6), and the pressure rise variable can be regarded invarant. For simplicity, the pressure ratio $R_p$ will be used in the remaining of the analysis, as pressure ratio and corrected pressure rise are equivalent when regarding invariance.

### 4.3.2 Surge control line

The surge control line is computed from the surge line, adding a margin in percentage of flow. This can be expressed by:

$$c(R_{p,SCL}) = [1 + b_1] j(R_{p,SL}) \tag{4.36}$$

$$\bar{q}_d = c(R_p)^2 \tag{4.37}$$

This synthesis is equal to the one presented for the first anti surge strategy.

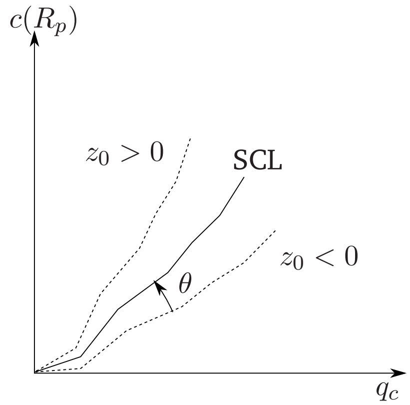


**Figure 4.9:** Interpretation of control variable.

### 4.3.3 Control variable structure

Control is based on the ratio between $\bar{q}$ and $\bar{q_d}$ in accordance with (4.4), which gives:

$$z = 1 - \frac{q_c^2}{c(R_p)^2} \tag{4.38}$$

The control variable can be viewed differently by including the relationship given by (3.23):

$$z = 1 - \frac{q_c^2}{c(R_p)^2} = 1 - \frac{q_c^2 c(R_{p,e})^2}{c(R_p)^2 q_e^2} = 1 - (\frac{(q_c/q_e)}{(c(R_p)/c(R_{p,e}))})^2 \tag{4.39}$$

From this it is seen that the control variable is constructed from the ratio between measured flow and flow at the equilibrium, and ratio between SCL values of measured pressure ratio and pressure ratio at the equilibrium.

Further, considering constant values $z = z_0 \leq 1$, the flow versus SCL is given by:

$$q_c = c(R_p)\sqrt{(1 - z_0)}$$

This structure resemble the effects illustrated in Figure 4.1, only applied on the SCL. Hence, the control variable describes the angle $\theta$ between a SCL with altered slope and the SCL, see Figure 4.9. If $z_0 = 0$, the operating point is on the SCL.

### 4.3.4 Control variable dynamics

To analyse the dynamics of the control variable, it is adapted to the framework from (3.20). The relationship from (4.38) is given by:

$$\begin{aligned} z = i(y) &= 1 - \frac{p_{ref} y_3}{y_1 c(\frac{y_2}{y_1})^2} \\ &= 1 - a_7 \frac{x_3^2/x_1^2}{c(\frac{x_2}{x_1})^2} \\ &= k(x) \end{aligned} \tag{4.40}$$

Further, including the dynamic coupling effects of the states from strategy 1 given by (4.24) and (4.25) gives:

$$
\begin{aligned}
z &= 1 - \frac{q_c^2}{c(\psi_c(\frac{q_c}{a_7}) - \frac{\dot{x_3}}{a_3 x_1})^2} \\
&= 1 - \frac{q_c^2}{c(\psi_c(\frac{q_c}{a_7}) - \frac{\dot{q_c}}{a_3 a_7} + q_c^2 \frac{a_1}{a_3 a_7^2} - q_c \frac{a_1}{a_3 a_7}(v_1/x_1 - x_4/x_1))^2}
\end{aligned} \tag{4.41}
$$

The derivation of this result is identical to the one used in the analysis of the first strategy. The damping term introduced by $\dot{q_c}$ appears in the denominator of (4.41), but its effects are similar to the ones mentioned in the first analysis. Fast variations of compressor flow may cause the recycle valve to be actuated, even if the operating point is to the right of the SCL.

**Derivative**

The second time derivative of the control variable is:

$$
\begin{aligned}
m(x,u,v) = L_f^2 k(x) + L_g L_f k(x) \frac{1}{u} + [L_{e_1} L_f k(x) + L_f L_{e_1} k(x)] v_1 + L_{e_2} L_f k(x) v_2 \\
+ {L_{e_1}}^2 k(x) v_1^2
\end{aligned} \tag{4.42}
$$

The structure of (4.42) is equal to the one given by (4.27), but the terms are altered. Nonetheless, the relative degree of two is preserved in this choice of control variable, which is expected as the same measurements are utilized in both strategies.

**Transfer function**

The linearization procedure given by (4.12) is performed on the current strategy, and the resulting transfer function is presented in Appendix C. The observations regarding the relative degree of the linearized system and the number of poles are similar to the ones presented for the first strategy. This is expected, as the pole placement is a system property which is unaffected by the choice of strategy, and the same system input $u$ and measurements $y$ are used.

The steady state gain is given by:

$$
N_u(0) = -2{a_7}^2 {v_2}^2 {R_{p,e}}^2 \left(R_{p,e} - 1\right)^2 \left(a_7 - \psi_c'(\frac{q_e}{a_7}) c'(R_{p,e})\right) \tag{4.43}
$$

$$
\begin{aligned}
D_u(0) = \left(v_2 c\left(R_{p,e}\right) - v_1 a_7 R_{p,e}\right) c\left(R_{p,e}\right) \Big[ \psi_c' \left(\frac{q_e}{a_7}\right) \Big( v_2 c\left(R_{p,e}\right) \\
- 2 v_2 R_{p,e} c\left(R_{p,e}\right) + v_1 a_7 R_{p,e} \Big) + 2 a_7 v_2 R_{p,e}(R_{p,e} - 1) \Big]
\end{aligned} \tag{4.44}
$$

The expression for the steady state gain is similar to the one given in (4.31). In fact, the only difference is the term $c(R_{p,e})$, which appears in the numerator of strategy 1 and the denominator of strategy 2. Referring to the steady state gain from strategy 1 as $H_{u,1}(0)$ and from strategy 2 as $H_{u,2}(0)$, we have:

$$\frac{H_{u,1}(0)}{H_{u,2}(0)} = c(R_{p,e})^2 \tag{4.45}$$

As the SCL described by $c(R_{p,e})$ is strictly increasing, the steady state gain from strategy 1 will be larger than strategy 2 when $c(R_{p,e}) = q_e > 1$. However, as mentioned the size of the steady state gain is not interesting by itself, and the scaling difference from (4.45) will be counteracted by integral effects in the controller. The rest of the analysis will be conducted by numerical example, using the same parameters as for strategy 1.

### Zeroes and poles

The system poles are independent of the proposed strategy. Consequently, the pole analysis for changing $R_{p,e}$ presented in 4.2.4 also applies for strategy 2, and will not be repeated. The placement and behaviour of the zeroes are also minimally affected by the change of control strategy, as seen in Figure 4.10. Consequently, the relative placement of the poles and zeros shown in 4.4 is still valid, along with the method of referring to poles and zero by their subscript from (4.32).

### Frequency analysis

Because the placement and movement of the zeros and poles are not significantly altered from strategy 1 to strategy 2, neither will the behaviour for increasing system input frequency shown in Figure 4.6. However, the figure does not illustrate very well the difference in gain encountered for increasing pressure ratios/speeds. For the latter analysis, the steady state gain of the system will give clearer indications.

### Steady state gain

The steady state gain of strategy 2 is shown in Figure 4.11. Like for strategy 1, the gain strictly increases for increasing pressure ratios, which implies that tuning should be performed for high compression ratios/speeds. However, the gain increase of 1.46 from lowest to highest value is significantly lower than strategy 1. Further, the Figures in 4.12 show the steady state gain change from the disturbances to system output, where $v_1$ is the inflow and $v_2$ is the downstream pressure. It is recognized that the steady state gain actually strictly decreases for increasing compressor speed, opposite of strategy 1. However the difference of 1.16 is not large, such that a given change in disturbance will give almost equal change in the control variable regardless of operating point of the compression system.

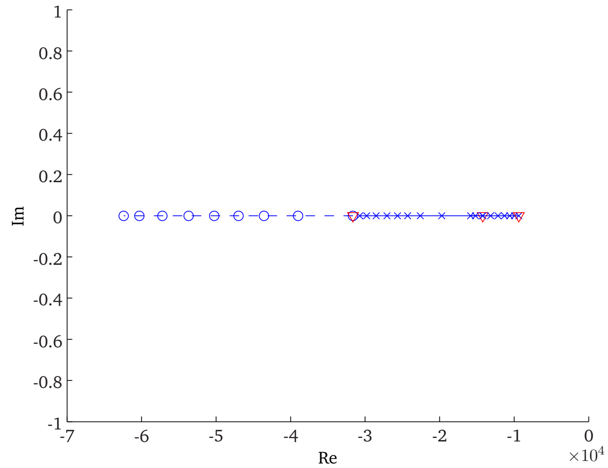


(a) 1,2,5

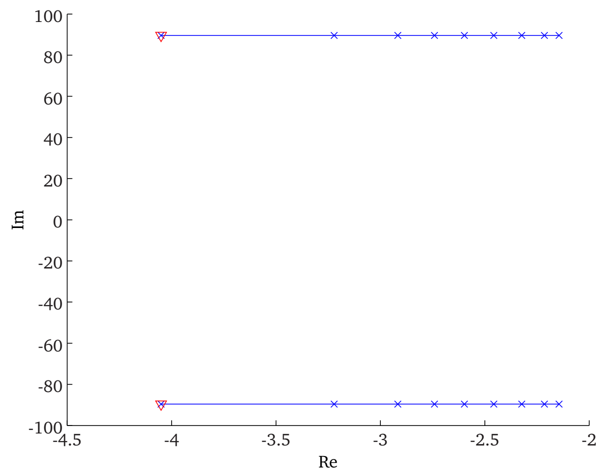


(b) 3

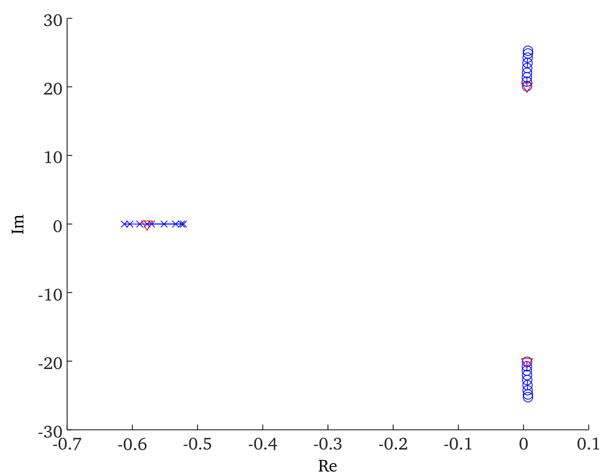


(c) 4,6

**Figure 4.10:** Movement of zeroes and poles, corresponding value for lowest $R_{p,e}$ marked by a red downward pointing triangle.

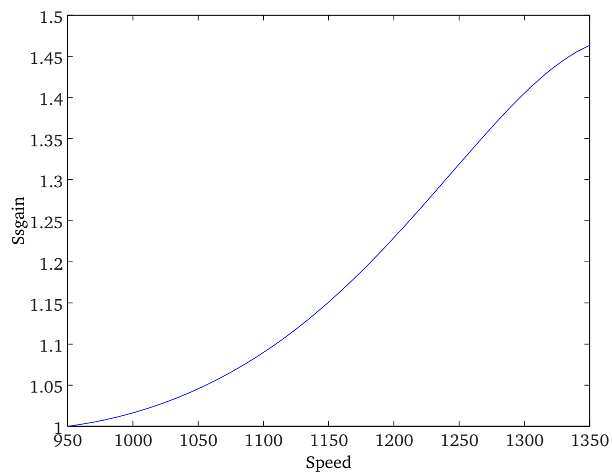


**Figure 4.11:** Normalized steady state gain for system input over a range of compressor speeds.

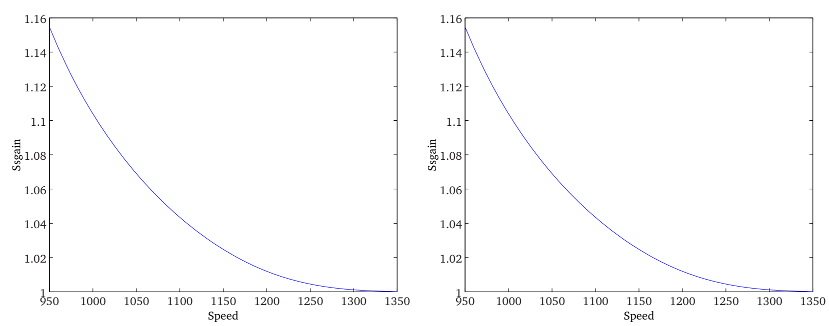


(a) $v_1$ (b) $v_2$

**Figure 4.12:** Normalized steady state gain for disturbances.

## 4.4 Summary

The reviewed strategies have both used parameters for their control variable synthesis regarded invariant with respect to the presented model. If temperature dynamics were included this would generally not be the case, however as previously discussed, temperature is usually regulated in compressor inlet.

Some considerations regarding the control variable structure and geometric interpretations have also been presented, with the aim of clarifing how it is related to the system equilibrium and the distance to the SCL. The distances are closely related to the shape of the SCL, which has been illustrated by example. Generally, the control variable must be adapted to the shape of the SCL if it is supposed to represent the shortest distance to surge.

The SCL is similarly described for both strategies, such that the margin to surge increases for increasing pressure ratios. Operation in the high speed region will therefore be able to withstand fast disturbances better than for the low speed region. This combined with the significant increase in input-output gain observed for strategy 1 will in practice cause deviations from SCL to be punished harder than for strategy 2 in the high speed area. For lower speeds, the smaller surge margin and input-output gain may be insufficient to withstand the compressor operating point entering surge. Strategy 2 will have similar response for the presented speeds.

Qualitative dynamic behaviour is from the pole-zero and frequency analysis recognized to be similar for both strategies. An increase in compressor speed implies faster or more oscillatory dynamics for all states.

### Flow and ratio control variable

From the expressions for the presented control variables given by (4.21) and (4.39), it is recognized that they both are constructed by a non linear mapping of the distance of the operating point to equilibrium. The contributions to the control variable from flow distance and ratio distance is implicitly defined by the SCL. It has also been shown that including measured compression ratio as input to the SCL, have the effect of including additional damping in the control system.

However, the SCL being responsible for the weighing of the flow distance and ratio distance may not be the obvious choice. The SCL could rather represent a safety margin only, such that tuning is decoupled from the definition of the SCL. A more flexible scheme for the control variable would e.g. be given by:

$$z = k_1(\Delta R_p) + k_2(\Delta q_c) \tag{4.46}$$

where $\Delta R_p = R_p - R_{p,e}$, $\Delta q_c = q_e - q_c$. The functions $k_1(\cdot)$ , $k_2(\cdot)$ are possibly non linear functions reflecting the operating points distance to the surge line for the compression ratio and flow along the along the corresponding axes. This scheme assumes that the equilibrium is known which is valid if the desired compressor speed is made available. The equilibrium can then be calculated via the SCL. On the downside, this would result in additional tuning parameters.

# Chapter 5

# Simulations

The model from (3.20) was implemented in MATLAB/Simulink ® to verify the various system and strategy properties previously presented. The same parameters used for the numerical analysis were employed, which are given in appendix A.

As shown in section 4.2.4, the compression system have parts of the dynamics which are significantly faster than others. This is the characteristic of a so called stiff system [22], requiring other numerical solvers than system simulations where the dynamics are less varying. The chosen algorithm was the ode15s, a variable order solver suited for stiff systems. For further reading, see the MATLAB Help file.

The time simulations have been performed by the following steps for a range of pressure ratios/compressor speeds:

1. Place the system state initial values in the equilibrium given by (3.24). This also means that the system input/valve opening differ for each speed.

2. Apply a pulse for one second on the input with a given percentage increase of the intial value.

3. Review response of control variable after pulse.

## 5.1 Strategy 1

### 5.1.1 System input pulse

The characteristic behaviour of the system for different speeds are shown in Figures 5.1. From Figure 5.1(a), it is first recognized that the valve opening strictly decreases for increasing speeds. The demanded increase in recycle flow is more than satisfied by the higher pressure ratios, such that the valve must be closed to remain on the SCL. This also means that the system input pulse amplitude is lower for increasing speeds.

The qualitative behaviour of the control variable for increasing speed is identical, which is seen from Figure 5.1(b). The behaviour can be characterized as combination a first order response, and an underdamped second order

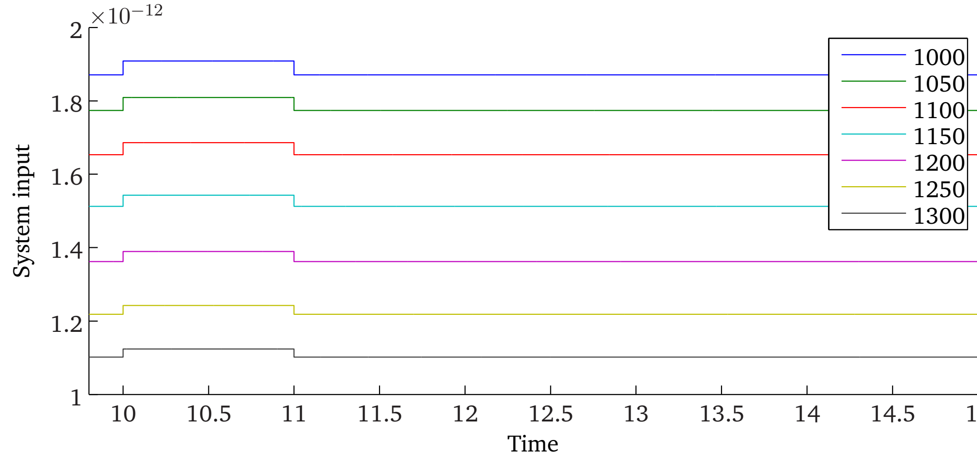


(a) System input pulse

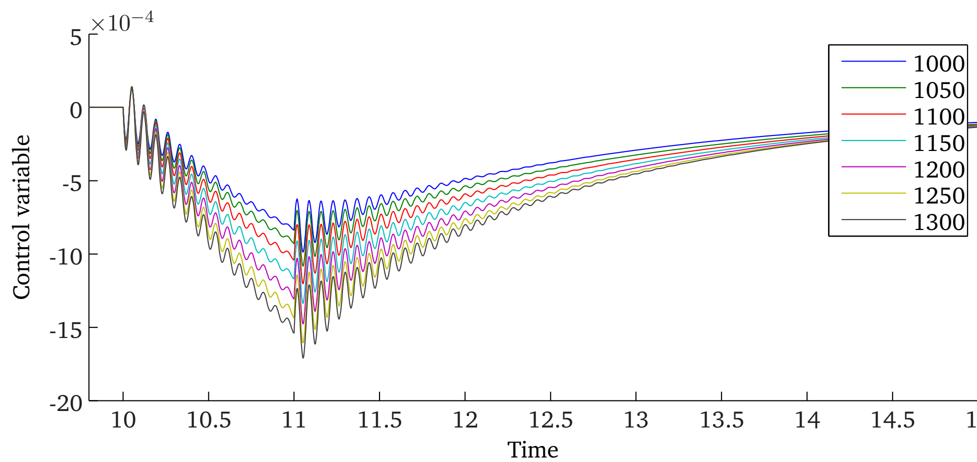


(b) Control variable response

**Figure 5.1:** Strategy 1 control variable response to pulse increase in system input of two percent. Colors represent the different compressor speeds.

response, where the second order dynamics are faster than the first order dynamics. The oscillation frequency is by closer inspection found to be around $90\,rad/s$. Further, it is seen that the response amplitude increases for increasing speed.

Referring to the zero and pole placement analysis in section 4.2.4, the contribution to the qualitative time response by poles $1$, $2$ and zero $5$ are unobservable due to the fast dynamics.

The first order response is therefore assosiated with pole $4$, while oscillations observed are caused by the pole pair $3$. Pole $4$ is smaller in absolute value than pair $3$, such that dynamics related to pole $4$ are slower than those related to pair $3$. The pair $3$ has a significantly larger imaginary than real part, implying that oscillations will be poorly damped. The observed oscillation frequency also corresponds well with the resonance frequency of pole pair $3$ of $90\,rad/s$. Consequently, the observed oscillations are caused by the check valve duct dynamics. The lack of damping terms in the modeling induces oscillations for rapid actuation of the recycle valve.

The increase in response amplitude of the control variable for increasing speed was antisipated by the steady state gain analysis. Even though the system input pulse amplitude actually diminish, the gain increase overcompensates the amplitude reduction. The gain increase is related to the negative slope in compressor map. For the equilibria on the SCL, the slope becomes more negative for increasing speeds. A small deviation from equilibrium will therefore cause a more vigorous response. The larger differential pressure for increasing speeds will also contribute to this behaviour.

### 5.1.2 Disturbance pulse

Simulations have also been performed where the disturbance feed flow has been given an impulse while keeping system input/valve opening constant. The results of these simulations are given in Figure 5.2. Figure 5.2(a) shows that the disturbance initial value and pulse is equal for all speeds, since the demanded increase in compressor flow is maintained by the increased differential pressure.

In Figure 5.2(b) it is seen that the asymptotic behaviour of the control variable is similar to the one caused by a pulse in system input. However, oscillations are not observed. The amplitude of control variable is much larger than response from the system input pulse, but in both cases there are increasing amplitude for increasing speed.

The large difference in amplitude for the disturbance pulse compared to the system input pulse are related to the amount the two pulsess inflict on total compressor flow. The recycle line flow is not only determined by valve opening, but also the differential pressure between volume 2 and volume 1. The feed flow on the other hand, is directly affected by the pulse.

The oscillations from the system input pulse does not appear, which is a consequence of where the pulse enter the system. The disturbance pulse initially affect the dynamics associated with volume 1, previously identified as the slowest dynamic component of the system. Therefore, all other system dynamics are able keep up with the changes inflicted on the volume 1 pressure, and faster dynamics are not excited by the disturbance pulse.

As the amplitude of the response increases for increasing speed, the control variable will react more severly to a given disturbance when operating in the high speed area. This corresponds well with the conclusions from the steady state gain analysis, and the response of the control variable to changes in system input.

## 5.2 Strategy 2

### 5.2.1 System input pulse

The previously described simulations where performed with the control variable from strategy 2, and the results are shown in Figure 5.3. The observations

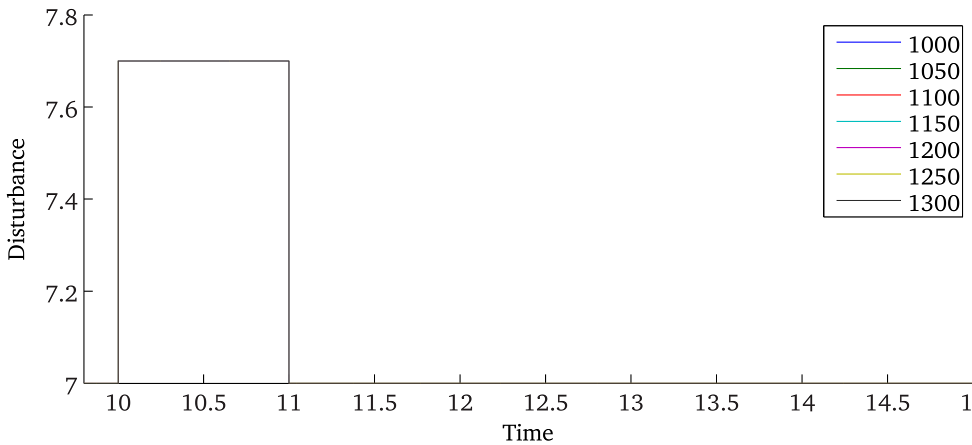


(a) Disturbance pulse

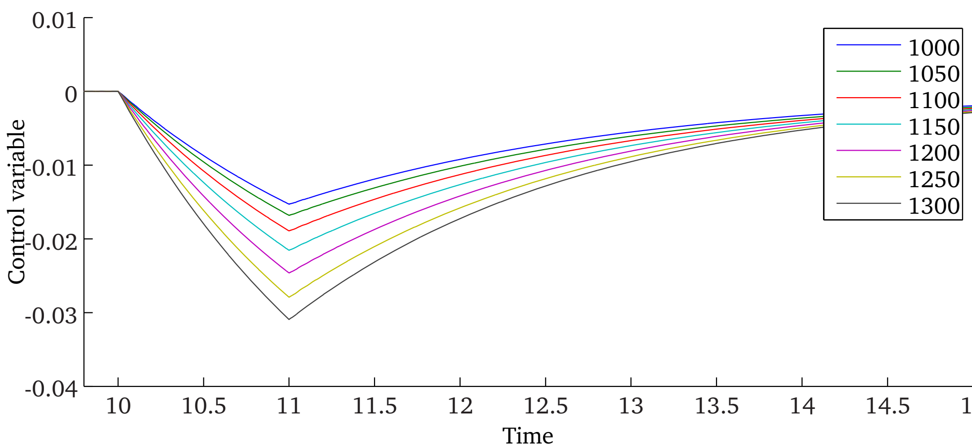


(b) Control variable response

**Figure 5.2:** Strategy 1 control variable response to pulse increase in disturbance $v_1$ of ten percent. Colors represent the different compressor speeds.

regarding the system input pulse are preserved from the strategy 1 analysis, as the same scheme is used. This also applies to the qualitative behaviour of the control variable for increasing speeds, and the relationships to the pole and zero placement. Hence, the observations and considerations presented for strategy 1 will not be repeated.

However, there are significant differences regarding the amplitude of the control variable response, and how this is affected by increasing speeds. The size of the amplitude is almost double of the one encountered in strategy 1. Further, the time response is almost equal for all compressor speeds.

The first obeservation implies that the overall gain from system input to control variable is higher compared to strategy 1. When used as input to a controller, the controller parameters should therefore be smaller than if the control variable from strategy 1 was used and the same performance was desired. The second observation regarding the small variations in time response for increasing speed is accordance with the result from the steady state gain analysis. In

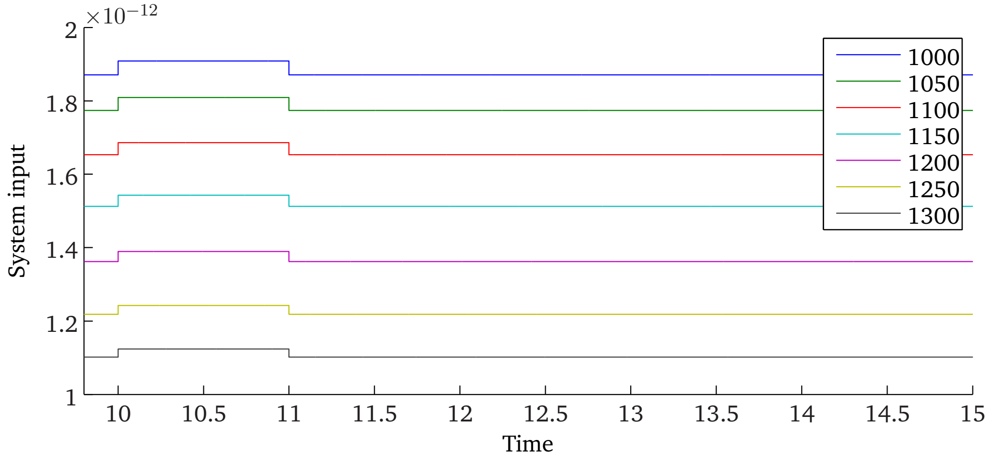


(a) System input pulse

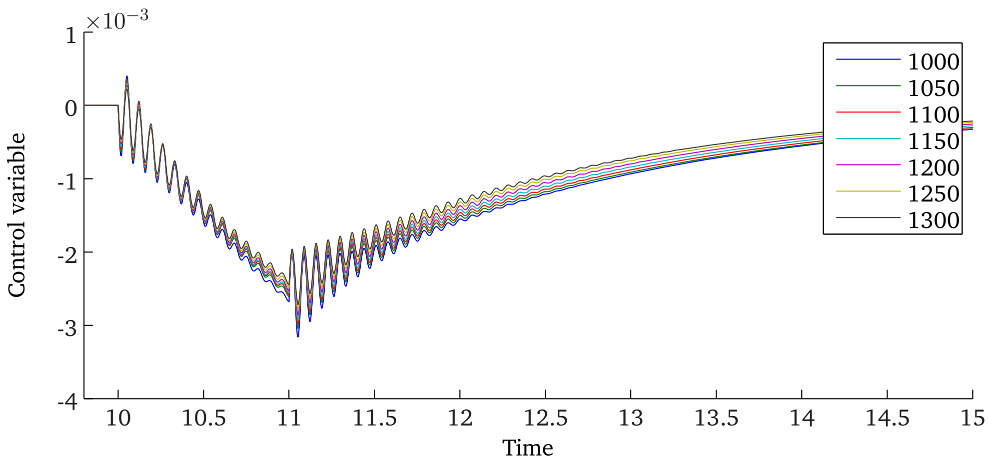


(b) Control variable response

**Figure 5.3:** Strategy 2 control variable response to pulse increase in system input of two percent. Colors represent the different compressor speeds.

fact, the response of the control variable is smaller for increasing speeds, but this is due to the decrease in pulse amplitude. Anyhow, the behaviour of the control variable to a given recycle valve change is almost equal for the whole speed range.

### 5.2.2 Disturbance pulse

Simulations have also been performed for pulses given to disturbance feed flow shown in 5.4. The qualitative behaviour of the control variable for different speeds is similar to the one encountered for strategy 1, and were previously explained. The control variable response amplitude is larger than for strategy 1, however it is almost equal for increasing speeds. Hence, control systems utilizing this strategy will react consistently to disturbance changes for the presented compressor speeds.

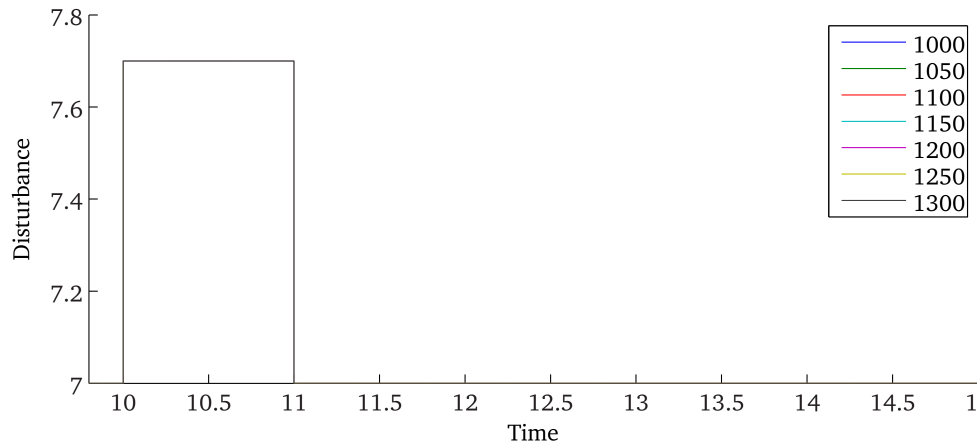


(a) Disturbance pulse

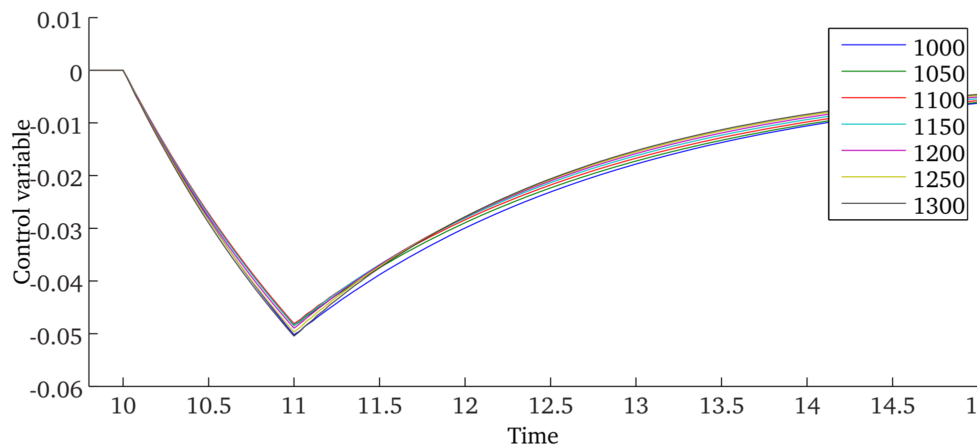


(b) Control variable response

**Figure 5.4:** Strategy 2 control variable response to pulse increase in disturbance $v_1$ of ten percent. Colors represent the different compressor speeds.

## 5.3 Summary

Most of the conclusions from the strategy analysis were validated through the performed simulations. The qualitative behaviour of the system related to pole and zero placement and frequency analysis were easily identified when simulating the non-linear model. This implies that the non-linearities of the system are not prominent for operating points close to the SCL and constant compressor speed.

However, the difference in input-output relationship, from system input or disturbance to control variable, between the various strategies were not easily identified through the pole placement and frequency analysis. Therefore, the steady state gain were used as a metric to describe the gain variations for a range of compressor speeds. These results also corresponded well with simulations.

Both the analysis and simulation suggest that the strategy 2 scheme will be less sensitive to speed changes, giving a more uniform response of the control variable, and that controller tuning should be performed for high compressor speeds. Valves with other characteristics than the linear will have their greatest amount of change when the initial valve opening is small. Other system parameters may give other results, but the main characteristics are believed to be maintained as long as the parameters are kept within certain boundaries.

# Chapter 6

# Conclusion

This thesis has presented a control theoretic approach to various aspects concerning anti surge control strategies. Especially, the structure of the control variable and input-output dynamics in open loop has been the main focus.

Chapter 1 gave a superficial introduction to compressors and anti surge control, followed by the motivation behind exploring the main characteristics of anti surge control strategies.

Chapter 2 presented the theory behind compressor and compressor control. A thorough review of the centrifugal compressor and its main properties was given. Further, the field of compressor control was presented, with special focus on anti surge control. Last, various aspects conserning the implementation of anti surge control strategies were discussed.

Chapter 3 derived a dynamic model representing the compressor and recycle line. This model was transformed into a framework suited for control theoretic analysis, followed by some important properties of the model.

Chapter 4 introduced the tools used to analyze anti surge control strategies, and presented some of the main implications caused by these tools. Later, two strategies were analyzed with respect to their structural and dynamic properties.

Chapter 5 validated the findings from chapter 4 by simulations.

The system was found to be open loop stable on the surge control line. The system dynamics were altered when compressor speed was changed. However, the qualitative response of the control variable was preserved for a different speeds and strategies. The main distinction between the speeds and strategies was found in the input-output gain. One strategy proved less affected by speed changes than the other. These findings were confirmed through simulations. The compression system model and also proved suitable for control theoretic analysis, however some of the aspects regarding the compression system and strategies were explored by numerical example.

## 6.1 Further work

The previously presented aspects concerning anti surge control and the synthesis of a control variable only cover some of the main system characteristics.

However, there are many loose ends and thoughts which are not explored. This section will present some of these, which hopefully can be the starting point for further investigations.

The focus of this thesis has been on the structural implications on the anti surge control variable, and dynamics in open loop. Consequently, control theoretic analysis of closed loop behaviour for different anti surge control strategies is a natural extension. There are many industrial implementations of anti surge control schemes which represent ad-hoc solutions not necessarily built on a analytic foundation. The implications of these solutions should be divided closer attention.

The close coupling between speed control and anti-surge control is especially interesting, due to the discussed relation to system equilibrium. In fact, the combination of the anti surge and the speed controller resembles the structure of a sliding mode controller. This controller structure will force the system to a given manifold or surface on which stability is ensured. On the manifold, the controller will actuate the system to reach a desired point. Related to the compression system, the manifold is given by the region to the right of the SCL. The anti surge controller forces the operating point of the compressor to this region. Further, the speed controller forces the operating point to an equilibrium on the speed line.

If viewing the compressor performance and protection in a wider perspective, the different goals represent a system ideal for a MPC [1] controller. The various actuation devices depicted could all be coordinated to optimize both compressor performance and protection. The SCL represents a constraint which for no circumstances should not be exceeded, whereas the performance controller has external set points defining desired compressor operation.

When it comes to stability related to the different compression system parameters, these may be evalutated by performing a bifurcation analysis. Parameters related to the anti-surge control scheme itself, such as recycle duct length, cross sectional area and valve coefficients, are of special interest. Synthesis of the SCL could also be further explored by this kind of analysis, e.g. choice of surge margin.

[1] Model Predictive Control.

# Bibliography


[1] M. P. Boyce, *Centrifugal compressors: a basic guide*. PennWell Books, 2003.

[2] B. de Jager, "Rotating stall and surge control: a survey," *Decision and Control, 1995., Proceedings of the 34th IEEE Conference on*, vol. 2, pp. 1857–1862 vol.2, Dec 1995.

[3] H. P. Bloch, *A practical guide to compressor technology*, 2nd ed. John Wiley and Sons, 2006.

[4] O. Banner, "Regulating mechanism for centrifugal compressors and pumps," U.S. Patent 1 222 352, April, 1917. [Online]. Available: http://www.freepatentsonline.com/1222352.html

[5] K. K. Botros and J. F. Henderson, "Developments in centrifugal compressor surge control—a technology assessment," *Journal of Turbomachinery*, vol. 116, no. 2, pp. 240–249, 1994. [Online]. Available: http://link.aip.org/link/?JTM/116/240/1

[6] I. Rutshtein, A1exander (West Des Moines and I. Staroselsky, Naum (West Des Moines, "Method and apparatus for antisurge protection of a dynamic compressor," U.S. Patent 4 046 490, September, 1977. [Online]. Available: http://www.freepatentsonline.com/4046490.html

[7] K. M. Eveker, D. L. Gysling, C. N. Nett, and H. O. Wang, "Compressor stall and surge control using airflow asymmetry measurement," U.S. Patent 5 915 917, June, 1999. [Online]. Available: http://www.freepatentsonline.com/5915917.html

[8] R. J. McKee, "A method for safely reducing surge margins in centrifugal compressors." Nashwille, Tennessee: GMRC Gas Machinery Conference, 2002.

[9] A. H. Epstein, J. E. F. Williams, and E. M. Greitzer, "Active suppression of aerodynamic instabilities in turbomachines," *Journal of Propulsion and Power*, vol. 5, no. 5, pp. 204–211, 1989.

[10] W. Blotenberg, "Process and device for the control of turbo compressors," U.S. Patent 4 944 652, July, 1990. [Online]. Available: http://www.freepatentsonline.com/4944652.html

[11] J.-L. Mondoloni, "Device for the control of anti-surge of a compressor," U.S. Patent 5 242 263, September, 1993. [Online]. Available: http://www.freepatentsonline.com/5242263.html

[12] L. D. McLeister, "Surge prevention control system for dynamic compressors," U.S. Patent 5 798 941, August, 1998. [Online]. Available: http://www.freepatentsonline.com/5798941.html

[13] N. Staroselsky, P. A. Reinke, and S. Mirsky, "Method and apparatus for preventing surge in a dynamic compressor," U.S. Patent EP0 500 196, June, 1994. [Online]. Available: http://www.freepatentsonline.com/EP0500196B1.html

[14] W. Blotenberg, "Process and device for regulating a turbocompressor to prevent surge," Germany Patent 6 558 113, May, 2003. [Online]. Available: http://www.freepatentsonline.com/6558113.html

[15] Siemens, "Compressor surge control using the model 352 single-loop controller," Moore Products CO, Tech. Rep., 1993. [Online]. Available: https://www2.sea.siemens.com/NR/rdonlyres/3D749CEF-8469-44E8-893B-98A0823136B6/0/ad352107.pdf

[16] J. R. Gaston, "Antisurge control system for compressors," U.S. Patent 5 195 875, March, 1993. [Online]. Available: http://www.freepatentsonline.com/5195875.html

[17] B. W. Batson, "Method and apparatus for antisurge control of turbocompressors having surge limit lines with small slopes," U.S. Patent 5 908 462, June, 1999. [Online]. Available: http://www.freepatentsonline.com/5908462.html

[18] L. Lorentzen, A. Hole, and T. Lindstrøm, *Kalkulus med én og flere variable*. Universitetsforlaget, 2003.

[19] O. A. Olsen, *Instrumenteringsteknikk*, 1994.

[20] R. W. Miller, *Flow Measurement Engineering Handbook*, 3rd ed. McGraw-Hill, 1996.

[21] P. Smith and R. W. Zappe, *Valve Selection Handbook*, 2004.

[22] O. Egeland and J. T. Gravdal, *Modeling and Simulation for Automatic Control*. Marine Cybernetics, 2003.

[23] C. Kleinstreuer, *Two-phase flow: thery and applications*. Taylor & Francis, 2003.

[24] E. W. Weisstein. (2009) Descartes' sign rule. Web. MathWorld–A Wolfram Web Resource. [Online]. Available: http://mathworld.wolfram.com/DescartesSignRule.html

[25] J. G. Balchen, T. Andresen, and B. A. Foss, *Reguleringsteknikk*, 2004, vol. 5.

[26] H. K. Khalil, *Nonlinear Systems*, 3rd ed. Prentice Hall, 2002.

[27] C.-T. Chen, *Linear System Theory and Design*, 3rd ed. Oxford University Press, 1999.

# Appendix A

# Numerical values

The compressor characteristics have been developed by curvefitting a third order polynomial to each of the speed lines from the compressormap in Figure 2.2. The lines have been extended into the negative flow region to such that the main behaviour in surge region is represented. Each of the speed line polynomial coefficients have then been fitted to third order polynomials using the centering and scaling procedure given by the MATLAB help file. This procedure can be described by:

$$\Psi_c(q_c, \omega) = c_3(\omega) q_c^3 + c_2(\omega) q_c^2 + c_1(\omega) q_c + c_0$$
$$c_x(\omega) = c_{x,3}\omega^3 + c_{x,2}\omega^2 + c_{x,1}\omega + c_{x,0}$$

The resulting compressor map and the SCL is shown in Figure A.1, data points are marked by a cross. The SCL has been synthesized according to (4.2), with slope parameter $c_0 = 0.6$.

Numerical values for the compression system parameters from (3.18) are presented in table A.1.

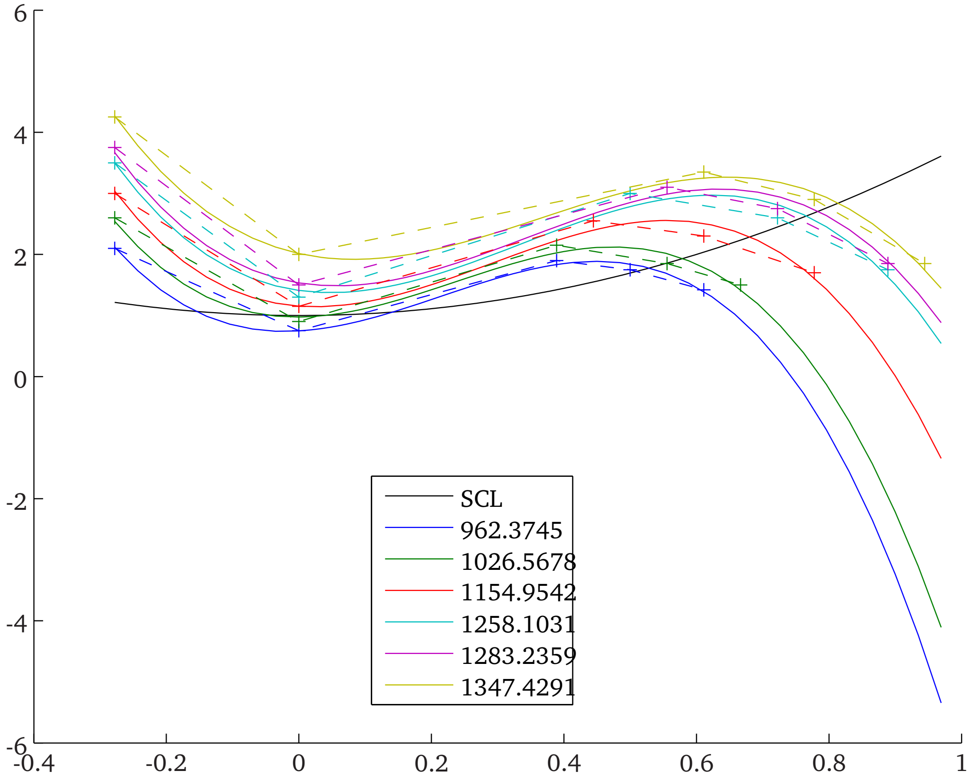


**Figure A.1:** Resulting compressor map after curvefitting.

| Symbol | Unit | Value |
|---|---|---|
| $M$ | $kg/mol$ | $22 * 10^{-3}$ |
| $R$ | $J/(mol \cdot K)$ | 8.314472 |
| $c_1$ | $m/s$ | 400.97 |
| $V_1$ | $m^3$ | 3.3 |
| $T_1$ | $K$ | 295.16 |
| $c_2$ | $m/s$ | 400.97 |
| $V_2$ | $m^3$ | 0.1 |
| $T_2$ | $K$ | 382.16 |
| $C_r^*$ | - | $3.1 * 10^{-3}$ |
| $L_c$ | $m$ | 10 |
| $A_c$ | $m^2$ | 0.5 |
| $L_r$ | $m$ | 50 |
| $A_r$ | $m^2$ | 0.5 |
| $L_t$ | $m$ | 100 |
| $A_t$ | $m^2$ | 0.5 |
| $J$ | $kg \cdot m^2$ | 2 |
| $r$ | $m$ | 0.29 |
| $w_f$ | $kg/s$ | 7 |
| $p_a$ | $Pa$ | $4 * 10^6$ |

**Table A.1**

# Appendix B

# Linearization

The linearized matrices of the system are given by:

$$A = \begin{bmatrix} 0 & 0 & -a_1 & a_1 & 0 \\ 0 & 0 & a_2 & -a_2 & -a_2 \\ a_3\left(\frac{\psi'(q_e/a_7)c(R_{p,e})}{a_7} + \psi(q_e/a_7)\right) & -a_3 & a_3\psi'(q_e/a_7) & 0 & 0 \\ -a_4 & a_4 + a_4(1 - 1/R_{p,e}) & 0 & -\frac{2a_4 v_2(1-1/R_{p,e})}{\frac{v_2 c(R_{p,e})}{a_7 R_{p,e}} - v_1} & 0 \\ 0 & a_5 & 0 & 0 & 0 \end{bmatrix}$$

$$B = \begin{bmatrix} 0 \\ 0 \\ 0 \\ \frac{a_4 v_2^3(1-1/R_{p,e})^2}{\left(\frac{v_2 c(R_{p,e})}{a_7 R_{p,e}} - v_1\right)^2} \\ 0 \end{bmatrix}$$

$$C_1 = \begin{bmatrix} 2\frac{c(R_{p,e})c'(R_{p,e}R_{p,e}^2) + c(R_{p,e})^2 R_{p,e}^2}{v_2} & \frac{2c(R_{p,e})c'(R_{p,e})R_{p,e}}{v_2} & \frac{-2a_7 c(R_{p,e})R_{p,e}}{v_2} & 0 & 0 \end{bmatrix}$$

$$C_2 = \begin{bmatrix} 2\frac{R_{p,e}}{v_2} - 2\frac{R_{p,e}^2 c'(R_{p,e})}{v_2 c(R_{p,e})} & \frac{2R_{p,e}^2 c'(R_{p,e})}{v_2 c(R_{p,e})} & \frac{-2a_7 R_{p,e}}{v_2 c(R_{p,e})} & 0 & 0 \end{bmatrix}$$

# Appendix C

# Transfer functions

$$\mathrm{D}(f)(x_e) = \frac{\partial f}{\partial x}|_{x=x_e}$$

## C.1 Strategy 1

$$N_u(s) = n_3 s^3 + n_2 s^2 + n_1 s + n_0$$

$$n_3 = -2\, a_4\, {v_2}^2 \left(R_{p,e} - 1\right)^2 \left(a_1\, \mathrm{D}(c)(R_{p,e})\, R_{p,e} - a_1\, c(R_{p,e}) + \mathrm{D}(c)(R_{p,e})\, a_2\right) {a_7}^3 c(R_{p,e})\, {R_{p,e}}^2$$

$$n_2 = -2\, a_4\, {v_2}^2 \left(R_{p,e} - 1\right)^2 \left(-a_1\, \mathrm{D}(c)(R_{p,e})\, R_{p,e}\, a_3\, \mathrm{D}(\psi_c)\left(\frac{c(R_{p,e})}{a_7}\right) + a_3\, a_2\, a_7 - \mathrm{D}(c)(R_{p,e})\, a_2\, \mathrm{D}(\psi_c)\left(\frac{c(R_{p,e})}{a_7}\right) a_3 + a_7\, a_3\, a_1\, R_{p,e}\right) {a_7}^3 c(R_{p,e})\, {R_{p,e}}^2$$

$$n_1 = -2\, a_4\, {v_2}^2 \left(R_{p,e} - 1\right)^2 \left(a_1\, \mathrm{D}(c)(R_{p,e})\, R_{p,e}\, a_5\, a_2 - a_1\, c(R_{p,e})\, a_5\, a_2\right) {a_7}^3 c(R_{p,e})\, {R_{p,e}}^2$$

$$n_0 = -2\, \left(R_{p,e} - 1\right)^2 {v_2}^2 a_4 \left(a_3\, a_5\, a_2\, a_1\, R_{p,e}\, a_7 - a_1\, \mathrm{D}(c)(R_{p,e})\, R_{p,e}\, a_5\, a_2\, \mathrm{D}(\psi_c)\left(\frac{c(R_{p,e})}{a_7}\right) a_3\right) {a_7}^3 c(R_{p,e})\, {R_{p,e}}^2$$

$$D_u(s) = d_5 s^5 + d_4 s^4 + d_3 s^3 + d_2 s^2 + d_1 s + d_0$$

$$d_5 = \left(-v_2 c(R_{p,e}) + v_1 a_7\, R_{p,e}\right)\left(-a_7\, R_{p,e}\, v_2 c(R_{p,e}) + {R_{p,e}}^2 {a_7}^2 v_1\right)$$

$$d_4 = \left(-v_2 c\left(R_{p,e}\right) + v_1 a_7\, R_{p,e}\right) \Bigg( R_{p,e}\, v_2 c\left(R_{p,e}\right) a_3\, \mathrm{D}\left(\psi_c\right) \left(\frac{c\left(R_{p,e}\right)}{a_7}\right) a_7 - v_1 {a_7}^2 {R_{p,e}}^2 a_3\, \mathrm{D}\left(\psi_c\right) \left(\frac{c\left(R_{p,e}\right)}{a_7}\right) - 2\, a_4\, {a_7}^2 v_2 {R_{p,e}}^2 + 2\, a_4\, {a_7}^2 v_2 R_{p,e} \Bigg)$$

$$\begin{aligned} d_3 = \left(-v_2 c\left(R_{p,e}\right) + v_1 a_7\, R_{p,e}\right) \Bigg( & 2\, a_4\, a_2\, v_1 {a_7}^2 {R_{p,e}}^2 + a_1\, {a_7}^2 a_3\, {R_{p,e}}^3 v_1 \\ & + R_{p,e}\, v_2 \left(c\left(R_{p,e}\right)\right)^2 a_3\, a_1\, \mathrm{D}\left(\psi_c\right) \left(\frac{c\left(R_{p,e}\right)}{a_7}\right) + a_4\, a_1\, v_1 {a_7}^2 {R_{p,e}}^2 \\ & - a_7\, a_5\, a_2\, R_{p,e}\, v_2 c\left(R_{p,e}\right) + a_4\, a_2\, v_2 c\left(R_{p,e}\right) a_7 + {a_7}^2 a_5\, a_2\, v_1 {R_{p,e}}^2 \\ & - R_{p,e}\, a_4\, a_1\, v_2 c\left(R_{p,e}\right) a_7 - 2\, a_4\, {a_7}^2 v_2 R_{p,e}\, a_3\, \mathrm{D}\left(\psi_c\right) \left(\frac{c\left(R_{p,e}\right)}{a_7}\right) \\ & - a_1\, a_7\, a_3\, {R_{p,e}}^2 v_2 c\left(R_{p,e}\right) + 2\, a_4\, {a_7}^2 v_2 {R_{p,e}}^2 a_3\, \mathrm{D}\left(\psi_c\right) \left(\frac{c\left(R_{p,e}\right)}{a_7}\right) \\ & + v_1 {a_7}^2 {R_{p,e}}^2 a_3\, a_2 - v_1 a_7\, {R_{p,e}}^2 a_3\, a_1\, \mathrm{D}\left(\psi_c\right) \left(\frac{c\left(R_{p,e}\right)}{a_7}\right) c\left(R_{p,e}\right) \\ & - R_{p,e}\, v_2 c\left(R_{p,e}\right) a_3\, a_2\, a_7 - a_4\, a_2\, v_1 {a_7}^2 R_{p,e} - 2\, a_4\, a_2\, v_2 R_{p,e}\, c\left(R_{p,e}\right) a_7 \Bigg) \end{aligned}$$

$$\begin{aligned} d_2 = \left(-v_2 c\left(R_{p,e}\right) + v_1 a_7\, R_{p,e}\right) \Bigg( & 2\, a_4\, a_7\, v_2 {R_{p,e}}^2 a_3\, a_1\, \mathrm{D}\left(\psi_c\right) \left(\frac{c\left(R_{p,e}\right)}{a_7}\right) c\left(R_{p,e}\right) \\ & + 2\, {a_7}^2 a_5\, a_2\, a_4\, v_2 R_{p,e} - a_4\, a_1\, v_1 {a_7}^2 {R_{p,e}}^2 a_3\, \mathrm{D}\left(\psi_c\right) \left(\frac{c\left(R_{p,e}\right)}{a_7}\right) \\ & - 2\, a_1\, {a_7}^2 {R_{p,e}}^3 a_4\, v_2 a_3 - a_4\, a_7\, v_2 R_{p,e}\, a_3\, a_1\, \mathrm{D}\left(\psi_c\right) \left(\frac{c\left(R_{p,e}\right)}{a_7}\right) c\left(R_{p,e}\right) \\ & + 2\, a_1\, {a_7}^2 {R_{p,e}}^2 a_4\, v_2 a_3 - 2\, {a_7}^2 a_5\, a_2\, a_4\, v_2 {R_{p,e}}^2 \\ & + 2\, a_4\, a_2\, v_2 R_{p,e}\, c\left(R_{p,e}\right) a_3\, \mathrm{D}\left(\psi_c\right) \left(\frac{c\left(R_{p,e}\right)}{a_7}\right) a_7 \\ & - 2\, a_4\, a_2\, v_1 {a_7}^2 {R_{p,e}}^2 a_3\, \mathrm{D}\left(\psi_c\right) \left(\frac{c\left(R_{p,e}\right)}{a_7}\right) \\ & + a_4\, a_2\, v_1 {a_7}^2 R_{p,e}\, a_3\, \mathrm{D}\left(\psi_c\right) \left(\frac{c\left(R_{p,e}\right)}{a_7}\right) + 2\, a_4\, {a_7}^2 v_2 R_{p,e}\, a_3\, a_2 \\ & - {a_7}^2 a_3\, a_5\, a_2\, \mathrm{D}\left(\psi_c\right) \left(\frac{c\left(R_{p,e}\right)}{a_7}\right) v_1 {R_{p,e}}^2 - 2\, a_4\, {a_7}^2 v_2 {R_{p,e}}^2 a_3\, a_2 \\ & - a_4\, a_2\, v_2 c\left(R_{p,e}\right) a_3\, \mathrm{D}\left(\psi_c\right) \left(\frac{c\left(R_{p,e}\right)}{a_7}\right) a_7 \\ & + a_7\, a_3\, a_5\, a_2\, \mathrm{D}\left(\psi_c\right) \left(\frac{c\left(R_{p,e}\right)}{a_7}\right) R_{p,e}\, v_2 c\left(R_{p,e}\right) \Bigg) \end{aligned}$$

$$d_1 = (-v_2 c(R_{p,e}) + v_1 a_7 R_{p,e}) \Big( a_1 a_7^2 a_3 R_{p,e}^3 a_5 a_2 v_1 + 2 a_7^2 a_3 a_5 a_2 \mathrm{D}(\psi_c)\left(\frac{c(R_{p,e})}{a_7}\right) a_4 v_2 R_{p,e}^2 - a_1 a_7 a_3 a_5 a_2 \mathrm{D}(\psi_c)\left(\frac{c(R_{p,e})}{a_7}\right) c(R_{p,e}) v_1 R_{p,e}^2 - a_1 a_7 a_5 a_2 R_{p,e} a_4 v_2 c(R_{p,e}) + a_1 a_7^2 a_5 a_2 a_4 v_1 R_{p,e}^2 + a_1 a_3 a_5 a_2 \mathrm{D}(\psi_c)\left(\frac{c(R_{p,e})}{a_7}\right)(c(R_{p,e}))^2 R_{p,e} v_2 - a_1 a_7 a_3 R_{p,e}^2 a_5 a_2 v_2 c(R_{p,e}) - 2 a_7^2 a_3 a_5 a_2 \mathrm{D}(\psi_c)\left(\frac{c(R_{p,e})}{a_7}\right) a_4 v_2 R_{p,e} \Big)$$

$$d_0 = (-v_2 c(R_{p,e}) + v_1 a_7 R_{p,e}) \Big( -a_1 a_7 a_3 a_5 a_2 \mathrm{D}(\psi_c)\left(\frac{c(R_{p,e})}{a_7}\right) c(R_{p,e}) a_4 v_2 R_{p,e} - 2 a_1 a_7^2 a_3 R_{p,e}^3 a_5 a_2 a_4 v_2 + 2 a_1 a_7^2 a_3 R_{p,e}^2 a_5 a_2 a_4 v_2 + 2 a_1 a_7 a_3 a_5 a_2 \mathrm{D}(\psi_c)\left(\frac{c(R_{p,e})}{a_7}\right) c(R_{p,e}) a_4 v_2 R_{p,e}^2 - a_1 a_7^2 a_3 a_5 a_2 a_4 v_1 R_{p,e}^2 \mathrm{D}(\psi_c)\left(\frac{c(R_{p,e})}{a_7}\right)\Big)$$

## C.2 Strategy 2

$$N_u(s) = n_3 s^3 + n_2 s^2 + n_1 s + n_0$$

$$n_3 = -2 a_4 v_2^2 (R_{p,e} - 1)^2 (a_1 \mathrm{D}(c)(R_{p,e}) R_{p,e} - a_1 c(R_{p,e}) + \mathrm{D}(c)(R_{p,e}) a_2) a_7^3 R_{p,e}^2$$

$$n_2 = -2 a_4 v_2^2 (R_{p,e} - 1)^2 \Big( -a_1 \mathrm{D}(c)(R_{p,e}) R_{p,e} a_3 \mathrm{D}(\psi_c)\left(\frac{c(R_{p,e})}{a_7}\right) + a_3 a_2 a_7 - \mathrm{D}(c)(R_{p,e}) a_2 \mathrm{D}(\psi_c)\left(\frac{c(R_{p,e})}{a_7}\right) a_3 + a_7 a_3 a_1 R_{p,e} \Big) a_7^3 R_{p,e}^2$$

$$n_1 = -2 a_4 v_2^2 (R_{p,e} - 1)^2 (a_1 \mathrm{D}(c)(R_{p,e}) R_{p,e} a_5 a_2 - a_1 c(R_{p,e}) a_5 a_2) a_7^3 R_{p,e}^2$$

$$n_0 = -2 a_4 v_2^2 (R_{p,e} - 1)^2 \Big( a_3 a_5 a_2 a_1 R_{p,e} a_7 - a_1 \mathrm{D}(c)(R_{p,e}) R_{p,e} a_5 a_2 \mathrm{D}(\psi_c)\left(\frac{c(R_{p,e})}{a_7}\right) a_3 \Big) a_7^3 R_{p,e}^2$$

$$D_u(s) = d_5 s^5 + d_4 s^4 + d_3 s^3 + d_2 s^2 + d_1 s + d_0$$

$$d_5 = c\left(R_{p,e}\right)\left(-v_2 c\left(R_{p,e}\right) + v_1 a_7\, R_{p,e}\right)\left(-a_7\, R_{p,e}\, v_2 c\left(R_{p,e}\right) + {R_{p,e}}^2 {a_7}^2 v_1\right)$$

$$\begin{aligned} d_4 = c\left(R_{p,e}\right)\left(-v_2 c\left(R_{p,e}\right) + v_1 a_7\, R_{p,e}\right)\Bigg( & R_{p,e}\, v_2 c\left(R_{p,e}\right) a_3\, \mathrm{D}\left(\psi_c\right)\left(\frac{c\left(R_{p,e}\right)}{a_7}\right) a_7 \\ & - v_1 {a_7}^2 {R_{p,e}}^2 a_3\, \mathrm{D}\left(\psi_c\right)\left(\frac{c\left(R_{p,e}\right)}{a_7}\right) - 2\, a_4\, {a_7}^2 v_2 {R_{p,e}}^2 + 2\, a_4\, {a_7}^2 v_2 R_{p,e}\Bigg) \end{aligned}$$

$$\begin{aligned} d_3 = c\left(R_{p,e}\right)\left(-v_2 c\left(R_{p,e}\right) + v_1 a_7\, R_{p,e}\right)\Bigg( & 2\, a_4\, a_2\, v_1 {a_7}^2 {R_{p,e}}^2 + a_1\, {a_7}^2 a_3\, {R_{p,e}}^3 v_1 \\ & + R_{p,e}\, v_2 \left(c\left(R_{p,e}\right)\right)^2 a_3\, a_1\, \mathrm{D}\left(\psi_c\right)\left(\frac{c\left(R_{p,e}\right)}{a_7}\right) + a_4\, a_1\, v_1 {a_7}^2 {R_{p,e}}^2 \\ & - a_7\, a_5\, a_2\, R_{p,e}\, v_2 c\left(R_{p,e}\right) + a_4\, a_2\, v_2 c\left(R_{p,e}\right) a_7 + {a_7}^2 a_5\, a_2\, v_1 {R_{p,e}}^2 \\ & - R_{p,e}\, a_4\, a_1\, v_2 c\left(R_{p,e}\right) a_7 - 2\, a_4\, {a_7}^2 v_2 R_{p,e}\, a_3\, \mathrm{D}\left(\psi_c\right)\left(\frac{c\left(R_{p,e}\right)}{a_7}\right) \\ & - a_1\, a_7\, a_3\, {R_{p,e}}^2 v_2 c\left(R_{p,e}\right) + 2\, a_4\, {a_7}^2 v_2 {R_{p,e}}^2 a_3\, \mathrm{D}\left(\psi_c\right)\left(\frac{c\left(R_{p,e}\right)}{a_7}\right) \\ & + v_1 {a_7}^2 {R_{p,e}}^2 a_3\, a_2 - v_1 a_7\, {R_{p,e}}^2 a_3\, a_1\, \mathrm{D}\left(\psi_c\right)\left(\frac{c\left(R_{p,e}\right)}{a_7}\right) c\left(R_{p,e}\right) \\ & - R_{p,e}\, v_2 c\left(R_{p,e}\right) a_3\, a_2\, a_7 - a_4\, a_2\, v_1 {a_7}^2 R_{p,e} - 2\, a_4\, a_2\, v_2 R_{p,e}\, c\left(R_{p,e}\right) a_7\Bigg) \end{aligned}$$

$$\begin{aligned} d_2 = c\left(R_{p,e}\right)\Big(-v_2 c\left(R_{p,e}\right) & \\ + v_1 a_7\, R_{p,e}\Big)\Bigg( & 2\, a_4\, a_7\, v_2 {R_{p,e}}^2 a_3\, a_1\, \mathrm{D}\left(\psi_c\right)\left(\frac{c\left(R_{p,e}\right)}{a_7}\right) c\left(R_{p,e}\right) \\ & + 2\, {a_7}^2 a_5\, a_2\, a_4\, v_2 R_{p,e} - a_4\, a_1\, v_1 {a_7}^2 {R_{p,e}}^2 a_3\, \mathrm{D}\left(\psi_c\right)\left(\frac{c\left(R_{p,e}\right)}{a_7}\right) \\ & - 2\, a_1\, {a_7}^2 {R_{p,e}}^3 a_4\, v_2 a_3 - a_4\, a_7\, v_2 R_{p,e}\, a_3\, a_1\, \mathrm{D}\left(\psi_c\right)\left(\frac{c\left(R_{p,e}\right)}{a_7}\right) c\left(R_{p,e}\right) \\ & + 2\, a_1\, {a_7}^2 {R_{p,e}}^2 a_4\, v_2 a_3 - 2\, {a_7}^2 a_5\, a_2\, a_4\, v_2 {R_{p,e}}^2 \\ & + 2\, a_4\, a_2\, v_2 R_{p,e}\, c\left(R_{p,e}\right) a_3\, \mathrm{D}\left(\psi_c\right)\left(\frac{c\left(R_{p,e}\right)}{a_7}\right) a_7 \\ & - 2\, a_4\, a_2\, v_1 {a_7}^2 {R_{p,e}}^2 a_3\, \mathrm{D}\left(\psi_c\right)\left(\frac{c\left(R_{p,e}\right)}{a_7}\right) \\ & + a_4\, a_2\, v_1 {a_7}^2 R_{p,e}\, a_3\, \mathrm{D}\left(\psi_c\right)\left(\frac{c\left(R_{p,e}\right)}{a_7}\right) + 2\, a_4\, {a_7}^2 v_2 R_{p,e}\, a_3\, a_2 \\ & - {a_7}^2 a_3\, a_5\, a_2\, \mathrm{D}\left(\psi_c\right)\left(\frac{c\left(R_{p,e}\right)}{a_7}\right) v_1 {R_{p,e}}^2 - 2\, a_4\, {a_7}^2 v_2 {R_{p,e}}^2 a_3\, a_2 \\ & - a_4\, a_2\, v_2 c\left(R_{p,e}\right) a_3\, \mathrm{D}\left(\psi_c\right)\left(\frac{c\left(R_{p,e}\right)}{a_7}\right) a_7 \\ & + a_7\, a_3\, a_5\, a_2\, \mathrm{D}\left(\psi_c\right)\left(\frac{c\left(R_{p,e}\right)}{a_7}\right) R_{p,e}\, v_2 c\left(R_{p,e}\right)\Bigg) \end{aligned}$$

$$
\begin{aligned}
d_1 = c\left(R_{p,e}\right)\left(-v_2 c\left(R_{p,e}\right) + v_1 a_7\, R_{p,e}\right) \Bigg( & a_1\; {a_7}^2 a_3\; {R_{p,e}}^3 a_5\; a_2\; v_1 \\
& + 2\, {a_7}^2 a_3\; a_5\; a_2\, \mathrm{D}\left(\psi_c\right)\left(\frac{c\left(R_{p,e}\right)}{a_7}\right) a_4\; v_2 {R_{p,e}}^2 \\
& - a_1\; a_7\; a_3\; a_5\; a_2\, \mathrm{D}\left(\psi_c\right)\left(\frac{c\left(R_{p,e}\right)}{a_7}\right) c\left(R_{p,e}\right) v_1 {R_{p,e}}^2 \\
& - a_1\; a_7\; a_5\; a_2\; R_{p,e}\; a_4\; v_2 c\left(R_{p,e}\right) + a_1\; {a_7}^2 a_5\; a_2\; a_4\; v_1 {R_{p,e}}^2 \\
& + a_1\; a_3\; a_5\; a_2\, \mathrm{D}\left(\psi_c\right)\left(\frac{c\left(R_{p,e}\right)}{a_7}\right)\left(c\left(R_{p,e}\right)\right)^2 R_{p,e}\, v_2 \\
& - a_1\; a_7\; a_3\; {R_{p,e}}^2 a_5\; a_2\; v_2 c\left(R_{p,e}\right) \\
& - 2\, {a_7}^2 a_3\; a_5\; a_2\, \mathrm{D}\left(\psi_c\right)\left(\frac{c\left(R_{p,e}\right)}{a_7}\right) a_4\; v_2 R_{p,e} \Bigg)
\end{aligned}
$$

$$
\begin{aligned}
d_0 = c\left(R_{p,e}\right)\left(-v_2 c\left(R_{p,e}\right) + v_1 a_7\, R_{p,e}\right) \Bigg( & a_1\; {a_7}^2 a_3\; {R_{p,e}}^3 a_5\; a_2\; v_1 \\
& + 2\, {a_7}^2 a_3\; a_5\; a_2\, \mathrm{D}\left(\psi_c\right)\left(\frac{c\left(R_{p,e}\right)}{a_7}\right) a_4\; v_2 {R_{p,e}}^2 \\
& - a_1\; a_7\; a_3\; a_5\; a_2\, \mathrm{D}\left(\psi_c\right)\left(\frac{c\left(R_{p,e}\right)}{a_7}\right) c\left(R_{p,e}\right) v_1 {R_{p,e}}^2 \\
& - a_1\; a_7\; a_5\; a_2\; R_{p,e}\; a_4\; v_2 c\left(R_{p,e}\right) + a_1\; {a_7}^2 a_5\; a_2\; a_4\; v_1 {R_{p,e}}^2 \\
& + a_1\; a_3\; a_5\; a_2\, \mathrm{D}\left(\psi_c\right)\left(\frac{c\left(R_{p,e}\right)}{a_7}\right)\left(c\left(R_{p,e}\right)\right)^2 R_{p,e}\, v_2 \\
& - a_1\; a_7\; a_3\; {R_{p,e}}^2 a_5\; a_2\; v_2 c\left(R_{p,e}\right) \\
& - 2\, {a_7}^2 a_3\; a_5\; a_2\, \mathrm{D}\left(\psi_c\right)\left(\frac{c\left(R_{p,e}\right)}{a_7}\right) a_4\; v_2 R_{p,e} \Bigg) c\left(R_{p,e}\right)\left(-v_2 c\left(R_{p,e}\right)\right. \\
& \left. + v_1 a_7\, R_{p,e}\right) \Bigg( -a_1\; a_7\; a_3\; a_5\; a_2\, \mathrm{D}\left(\psi_c\right)\left(\frac{c\left(R_{p,e}\right)}{a_7}\right) c\left(R_{p,e}\right) a_4\; v_2 R_{p,e} \\
& - 2\, a_1\; {a_7}^2 a_3\; {R_{p,e}}^3 a_5\; a_2\; a_4\; v_2 + 2\, a_1\; {a_7}^2 a_3\; {R_{p,e}}^2 a_5\; a_2\; a_4\; v_2 \\
& + 2\, a_1\; a_7\; a_3\; a_5\; a_2\, \mathrm{D}\left(\psi_c\right)\left(\frac{c\left(R_{p,e}\right)}{a_7}\right) c\left(R_{p,e}\right) a_4\; v_2 {R_{p,e}}^2 \\
& - a_1\; {a_7}^2 a_3\; a_5\; a_2\; a_4\; v_1 {R_{p,e}}^2 \mathrm{D}\left(\psi_c\right)\left(\frac{c\left(R_{p,e}\right)}{a_7}\right) \Bigg) \Bigg)
\end{aligned}
$$

# Appendix D

# CD content

The attached CD contains the Simulink model used to run the presented simulations, along with scripts developed to describe the compressor map and strategies. To run, start MATLAB/Simulink and execute the file initConstants3 before starting the simulation.

The files included are:

| Name | Function |
|---|---|
| initConstants3.m | Initializes all constants and finds equilibria |
| initCompressor3.m | Creates compressormap from given data points |
| recycle_controller.m | Computes the control variable |
| compressorMap3.m | Computes the pressure ratio for given inlet pressure and mass flow |
| eq_fun.m | Finds the crossing between the SCL and the desired speed line |
| SCL.m | Give desired flow from desired pressure ratio |
| SCLinv.m | Give desired pressure ratio from desired flow |
| compressorV13openloop.mdl | The Simulink model for the compression system |